Exploring the structural, electronic and optical properties of the double perovskites Ca_2GaAsO_6 by first-principles study

Course Title : Thesis
Course Code : TPG-599

Submitted by
Exam Roll : 106714
Academic Year : 2020-21
Registration Number : 2016-118-722

Report submitted to the Department of Theoretical Physics at
University of Dhaka
in partial fulfillment of the requirements
for the degree of Master of Science (MS).

July 2023

Abstract

This thesis explores the structural, electronic and optical properties of the double perovskites compound Ca_2GaAsO_6 using first-principles calculations. By employing density functional theory (DFT) within the framework of the generalized gradient approximation (GGA) and modified Becke Johnson (mBJ), electronic band structure of Ca_2GaAsO_6 are investigated. Here, the crystal structure of Ca_2GaAsO_6 is examined, with emphasis on the arrangement and coordination of the constituent atoms. The electronic properties of Ca_2GaAsO_6 are studied to gain insights into its potential for electronic applications. The density of states (DOS) is calculated, providing information on the energy bandgap. The dielectric function, optical absorption coefficient, optical reflectivity, optical conductivity and refractive index are calculated, allowing for the evaluation of the compound's response to light across a wide range of energies. The results obtained from these first-principles calculations provide valuable insights into the structural stability, electronic band structure and optical properties of Ca_2GaAsO_6. The findings contribute to the fundamental understanding of double perovskites materials and provide a basis for potential applications in optoelectronics, photonics and energy related technologies.

Acknowledgements

I would like to acknowledge the divine blessings and extol the greatness of Allah throughout this research journey. His boundless mercy and guidance have been a source of strength and inspiration, enabling me to overcome challenges and stay focused on my objectives.

I would also like to express my deepest gratitude and appreciation to Dr. Mohammad Abdur Rashid, Department of Physics at Jashore University of Science and Technology. His invaluable guidance, unwavering support and immense knowledge have been instrumental in the completion of this thesis.

I am grateful to my family and friends for their unwavering support, encouragement, and understanding during this arduous endeavor. Their love and belief in my abilities have been the driving force behind my success.

I am indebted to all those mentioned above, as well as those who have contributed to this work in various ways but may not be explicitly named. Without their collective efforts and contributions, this thesis would not have been possible.

Abu Raihan

Contents

Exploring the structural, electronic and optical properties of the double perovskites Ca_2GaAsO_6 by first-principles study

List of Figures

Exploring the structural, electronic and optical properties of the double perovskites Ca_2GaAsO_6 by first-principles study

Chapter 1

Introduction

The need for energy has significantly increased in recent years, which has accelerated efforts to identify non-fossil fuel and non-conventional energy sources [1]. In the past decade, due to the variety of applications of double perovskites oxides, especially their great use in energy production devices, they have attracted great interest from both theoretical and experimental points of view. Over recent years, double perovskites (DP) materials have attracted much attention due to their promising applications in different fields, such as light-emitting diodes (LEDs), lasers, radiation detectors and solar cells. Among different types of double perovskites, lead-based DP materials exhibit exceptional applications in photovoltaic technologies which are due to their suitable direct band gap, high absorption properties, and charge carriers' effective masses. [2–4]

To understand technological applications, such as solar panel manufacturing, photonic sensors, thermoelectric generators, luminescence, etc., it is compulsory to evaluate the performance of materials and their native properties [5]. The efficiency of oxide perovskites solar cells raised form 3.8 percent in 2009 to 26.08 percent in 2022 [6]. This is the best efficiency enhancement trend in the history of photovoltaics. Despite of remarkably high efficiency and low cost these champions have few disadvantages. The main problems with these organic-inorganic perovskites so-

lar cells are use of lead in their fabrication and stability issues. Lead is a toxic element and could be harmful for the human body and environment [7–9]. Lead can easily be dissolved and oxidize with the water molecules. Therefore, the installation of these solar cells with lead element in their fabrication could lead a serious threat to the environment and the existence of human population.

The double perovskitess fundamental structure is $A_2BB'O_6$ [10]. Here A is an alkaline-earth or rare-earth ion. The transition-metal sites (perovskites B-sites) are occupied alternately by different cations B and B$'$. Intervening oxygen bridges every B and B$'$ atom pair, thus forming alternating BO_6 and $B'O_6$ octahedra. This type of compound most of the time forms perfectly cubic structures with the space group no 225($Fm\bar{3}m$).

Double perovskitess are multipurpose materials. They have a wide range of sustainable and renewable applications because of their surprising stability and electronic structure. The distinctive features, such as hole and electron transport, high mobility and long diffusion lengths of the charge carrier, tunable bandgaps and stimulus-based variation in the properties, are the fundamentals of the notable performance of halide double perovskitess [11].

Research on double perovskites oxides has been extensive and has covered a wide range of topics. Here are a few areas where research has been conducted:

Magnetism and Spintronics: Double perovskites oxides have attracted significant attention for their magnetic properties and their potential applications in spintronics. For example, researchers have studied materials like Sr_2FeMoO_6, which exhibit colossal magnetoresistance, a large change in electrical resistance in response to an applied magnetic field. These materials are being explored for their potential use in magnetic sensors, magnetic memory devices, and spintronic applications [12–15].

Multiferroics: Multiferroic materials exhibit both ferroelectric and magnetic properties, which make them promising for applications in devices that can be controlled by both electric and magnetic fields. Double perovskites oxides have been studied for their multiferroic behavior, where researchers have investigated the coupling between the magnetic and ferroelectric properties. Materials such as Bi_2FeCrO_6 and Bi_2FeMnO_6 have been explored for their multiferroic properties [16–19].

Catalysis: Double perovskites oxides have shown potential as catalysts for various chemical reactions. Researchers have investigated their use in catalyzing oxygen reduction reactions (ORR) and oxygen evolution reactions (OER) for energy conversion and storage applications. Materials like La_2NiMnO_6 and La_2NiCoO_6 have been studied for their catalytic properties [20–23].

Thermoelectrics: Thermoelectric materials can convert waste heat into electricity, making them attractive for energy harvesting applications. Double perovskites oxides have been studied for their thermoelectric properties. Researchers have explored materials like Sr_2FeMoO_6 and Ba_2NaOsO_6 for their potential use in thermoelectric devices [24].

Superconductivity: Double perovskites oxides have also been investigated for their superconducting properties. For example, researchers have studied materials like Sr_2RuO_4 and Sr_2VO_3FeAs, which exhibit unconventional superconductivity at low temperatures. Understanding the superconducting behavior of these materials can shed light on the mechanisms behind high-temperature superconductivity [25–29].

These are just a few examples of the research conducted with double perovskites oxides. The field is broad, and ongoing research continues to explore their unique properties and potential applications in various fields of science and technology.

However, the unstable structure, high humidity, and environmental pollution of the lead-based DPs limit their practical applications. Therefore, in recent years, finding stable and nature-friendly non-toxic DP materials has been considered as a strategically important field of study.

The aim of this thesis is to explore the structural, electronic, and optical properties of Ca_2GaAsO_6 using a first-principles approach. By employing DFT calculations, we will unravel the underlying atomic and electronic structure of Ca_2GaAsO_6, investigate its stability, and analyze its electronic band structure. Furthermore, we will delve into the optical properties of Ca_2GaAsO_6, such as its absorption and emission spectra, to gain insights into its potential applications in optoelectronic devices.

To accomplish these objectives, this thesis will be organized as follows. In Chapter 2, we will provide an overview of the theoretical background and methodology.

Chapter 3 will focus on the a brief introduction to DFT and its application in material science.Finally, in Chapter 4, we will investigate the electronic properties of Ca_2GaAsO_6, examining its band structure, density of states, and electronic charge distribution and optical properties of Ca_2GaAsO_6, highlighting its absorption and emission characteristics.

By delving into the structural, electronic, and optical properties of Ca_2GaAsO_6, this thesis aims to provide valuable insights into the fundamental aspects of this double perovskites compound. The findings presented here will contribute to the understanding of its potential applications in advanced electronic and optoelectronic devices, and pave the way for future experimental investigations and materials design based on the unique properties of Ca_2GaAsO_6.

Chapter 2

Theoretical Background

Theoretical understanding of the electronic structure of chemical compounds and the processes, thermodynamics, and kinetics of chemical reactions may be achieved through the application of quantum mechanics. Although there are certain macroscopic systems to which it is directly applicable, it may be regarded of broadly as the study of physics on very small length scales. It describes how matter responds and interacts with energy on a scale of atoms and subatomic particles. The most fundamental forms that are relevant to many-body systems are covered in this chapter along with fundamental ideas and expressions. The Schrödinger equation, a specific wave equation, controls how quantum physics particles behave when they exhibit wavelike features. The Schrödinger equation is unique from the other wave equations in a few respects. All of our standard methods for resolving a wave equation and handling the answers remain valid despite these adjustments.

2.1 Schrödinger Equation

Schrödinger equation is basically a differential equation and widely used to solve problems based on the atomic structure of matter which is one of the most fundamental equations of quantum physics. The Schrödinger wave equation defines how

a particle behaves in a field of force or how a physical parameter changes over time. The equation is named after Erwin Schrödinger, who postulated the equation in 1925 and published it in 1926, forming the basis for the work that resulted in his Nobel Prize in Physics in 1933.
Conceptually, the Schrödinger equation is the quantum counterpart of Newton's second law in classical mechanics. Given a set of known initial conditions, Newton's second law makes a mathematical prediction as to what path a given physical system will take over time. The Schrödinger equation gives the evolution over time of a wave function, the quantum-mechanical characterization of an isolated physical system.

2.2 Time Dependent Schrödinger Equation

The form of the Schrödinger equation depends on the physical situation. The most general form is the time-dependent Schrödinger equation, which gives a description of a system evolving with time.

The time dependent schrödinger equation [30] is represented as

$$i\hbar\frac{\partial}{\partial t}\Psi(\vec{r},t) = \hat{H}\Psi(\vec{r},t) \tag{2.1}$$

It is often impracticable to use a complete relativistic formulation of the formula; therefore Schrödinger himself postulated a non-relativistic approximation which is nowadays often used, especially in quantum chemistry.
For a single particle, the Hamiltonian

$$\hat{H} = \hat{T} + \hat{V} = -\frac{\hbar^2}{2m}\vec{\nabla}^2 + V(\vec{r},t) \tag{2.2}$$

leads to the (non-relativistic) time-dependent single-particle Schrödinger equation

$$i\hbar\frac{\partial}{\partial t}\Psi(\vec{r},t) = [-\frac{\hbar^2}{2m}\vec{\nabla}^2 + V(\vec{r},t)]\Psi(\vec{r},t) \tag{2.3}$$

For N particles in three dimensions, the Hamiltonian is

$$\hat{H} = \sum_{i=1}^{N}\frac{\hat{p_i^2}}{2m_i} + V(\vec{r_1},\vec{r_2},....,\vec{r_N},t) = -\frac{\hbar^2}{2}\sum_{i=1}^{N}\frac{1}{m_i} + V(\vec{r_1},\vec{r_2},....,\vec{r_N},t) \tag{2.4}$$

The corresponding Schrödinger equation reads

$$i\hbar\frac{\partial}{\partial t}\psi(\vec{r_1},\vec{r_2},....,\vec{r_N},t) = [-\frac{\hbar^2}{2}\sum_{i=1}^{N}\frac{1}{m_i}\vec{\nabla_i^2} + V(\vec{r_1},\vec{r_2},....,\vec{r_N},t)]\psi(\vec{r_1},\vec{r_2},....,\vec{r_N},t) \tag{2.5}$$

The solutions of the time-independent Schrödinger equation are special cases, where the Hamiltonian itself has no time-dependency (which implies a time independent potential $V(\vec{r_1},\vec{r_2},...,\vec{r_N})$, and the solutions therefore describe standing waves which are called stationary states or orbitals).

The time-independent equation is obtained by the approach of separation of variables, i.e. the spatial part of the wave function is separated from the temporal part [31]

$$\Psi(\vec{r_1},\vec{r_2},....,\vec{r_N},t) = \psi(\vec{r_1},\vec{r_2},....,\vec{r_N},t)\tau(t) = \psi(\vec{r_1},\vec{r_2},....,\vec{r_N},t)e^{-i\omega t} \tag{2.6}$$

Furtheremore, the left hand side of the equation reduces to the energy eigenvalue of the Hamiltonian multiplied by the wave function, leading to the general eigenvalue equation

$$E\psi(\vec{r_1},\vec{r_2},...,\vec{r_N}) = \hat{H}\psi(\vec{r_1},\vec{r_2},...,\vec{r_N}) \tag{2.7}$$

Again, using the many-body Hamiltonian, the Schrödinger equation becomes

$$E\psi(\vec{r_1},\vec{r_2},...,\vec{r_N}) = [-\frac{\hbar^2}{2}\sum_{i=1}^{N}\frac{1}{m_i}\vec{\nabla_i^2} + V(\vec{r_1},\vec{r_2},....,\vec{r_N},t)]\psi(\vec{r_1},\vec{r_2},....,\vec{r_N},t) \tag{2.8}$$

2.3 The Wave Function

In quantum physics, a wave function is a mathematical description of the quantum state of an isolated quantum system. The wave function is a complex-valued probability amplitude, and the probabilities for the possible results of measurements made on the system can be derived from it. The first and most important postulate is that the state of a particle is completely described by its (time-dependent) wave function, i.e. the wave function contains all information about the particle's state. For the sake of simplicity the discussion is restricted to the time-independent wave function. A question always arising with physical quantities is about possible interpretations as well as observations. The Born probability interpretation of the wave function, which is a major principle of the Copenhagen interpretation of quantum mechanics, provides a physical interpretation for the square of the wave function as a probability density [32]

$$|\psi(\vec{r_1}, \vec{r_2}, \vec{r_3}, .., \vec{r_N}|^2 d\vec{r_1} d\vec{r_2} .... d\vec{r_N} \tag{2.9}$$

This equation describes the probability that particles 1,2,...,N are located simultaneously in the corresponding volume element $d\vec{r_1} d\vec{r_2} .... d\vec{r_N}$ [33]. What happens if the positions of two particles are exchanged, must be considered as well. Following merely logical reasoning, the overall probability density cannot depend on such an exchange, i.e.

$$|\psi(\vec{r_1}, \vec{r_2}, \vec{r_3}, ..., \vec{r_i}, \vec{r_j}, ..., \vec{r_N}|^2 = |\psi(\vec{r_1}, \vec{r_2}, \vec{r_3}, ..., \vec{r_j}, \vec{r_i}, ..., \vec{r_N}|^2 \tag{2.10}$$

The wave function's behavior during a particle exchange has just two possible outcomes. The first one is a symmetrical wave function, which does not change due to such an exchange. This corresponds to bosons (particles with integer or zero spin). The other possibility is an anti-symmetrical wave function, where an exchange of two particles causes a sign change, which corresponds to fermions (particles which half-integer spin). In this text only electrons are from interest, which are fermions [34].

The anti-symmetric fermion wave function leads to the Pauli principle, which states that no two electrons can occupy the same state, whereas state means the orbital and spin parts of the wave function [35]. The antisymmetry principle can be seen as the quantum mechanical formalization of Pauli's theoretical ideas in the description of spectra (e.g. alkaline doublets). Another consequence of the probability interpretation is the normalization of the wave function. If equation (2.9) describes the probability of finding a particle in a volume element,setting the full range of coordinates as volume element must result in a probability of one, i.e. all particles must be found somewhere in space. This corresponds to the normalization condition for the wave function.

$$\int d\vec{r_1} \int d\vec{r_2} ... \int d\vec{r_N} |\psi(\vec{r_1}, \vec{r_2}, \vec{r_3}, .., \vec{r_N}|^2 = 1 \tag{2.11}$$

Equation (2.11) also gives insight on the requirements a wave function must fulfill in order to be physical acceptable. Wave functions must be continuous over the full spatial range and square-integratable [35]. Another very important property of the wave function is that calculating expectation values of operators with a wave function provides the expectation value of the corresponding observable for that wave function. For an observable $O(\vec{r_1}, \vec{r_2}, ..., \vec{r_N})$ this can generally be written as

$$< O >= \int d\vec{r_1} \int d\vec{r_2} ... \int d\vec{r_N} \psi^*(\vec{r_1}, \vec{r_2}, .., \vec{r_N}) \hat{O} \psi^(\vec{r_1}, \vec{r_2}, .., \vec{r_N}) \tag{2.12}$$

2.4 Many Body System And Born Oppenheimer Approximation

The Hamiltonian of a many-body system consisting of nuclei and electrons can be written as [36]

$$H_{tot} = -\sum_{I} \frac{\hbar^2}{2M_I} \vec{\nabla^2_{\boldsymbol{R_I}}} - \sum_{i} \frac{\hbar^2}{2M_e} \vec{\nabla^2_{\boldsymbol{r_i}}} + \frac{1}{2} \sum_{I,J} \frac{Z_I Z_J e^2}{|\boldsymbol{R_I} - \boldsymbol{R_J}|} + \frac{1}{2} \sum_{i,j} \frac{e^2}{|\boldsymbol{r_i} - \boldsymbol{r_j}|} - \sum_{I,i} \frac{Z_I e^2}{|\boldsymbol{R_I} - \boldsymbol{r_i}|}$$

(2.13)

where the indexes I, J run on electrons, $\boldsymbol{R_I}$ and M_I are positions and masses of the nuclei, $\boldsymbol{r_i}$ and Me of the electrons, Z_I the atomic number of number of nucleus I. The first term is the kinetic energy of the nuclei, the second term is the kinetic energy of the electron, the third term is the potential energy of nucleus-nucleus Coulomb interaction, the fourth term is the potential energy of electron-electron Coulomb interaction and the last term is the potential energy of nucleus-electron Coulomb interaction [37]. The time-independent Schrödinger equation for the system :

$$H_{tot}\Psi = (\{\boldsymbol{R_I}\}, \{\boldsymbol{r_i}\}) = E\psi(\{\boldsymbol{R_I}\}, \{\boldsymbol{r_i}\}) \tag{2.14}$$

where $\psi(\{\boldsymbol{R_I}\}, \{\boldsymbol{r_i}\})$ is the total wavefunction of the system. Everything about the system is known if one can solve the above Schrödinger equation. However, it is impossible to solve it in practice. A so-called Born-Oppenheimer (BO) approximation was made by Born and Oppenheimer [38] in 1927. Since the nuclei are much heavier than electrons, the nuclei move much slower than the electrons. Therefore we can separate the movement of nuclei and electrons. When we consider the movement of electrons, it is responsible to consider the positions of nuclei are fixed, thus the total wavefunction can be written as:

$$\psi(\{\boldsymbol{R_I}\}, \{\boldsymbol{r_i}\}) = \Theta(\{\boldsymbol{R_I}\})\phi(\{\boldsymbol{r_i}\}; \{\boldsymbol{R_i}\}) \tag{2.15}$$

where $\Theta\{\boldsymbol{R_I}\}$ describes the nuclei and $\phi(\{\boldsymbol{r_i}\}; \{\boldsymbol{R_i}\})$ the electrons. With the BO

approximation, Eq. can be divided into two separate Schrödinger equations:

$$H_e\phi(\{\boldsymbol{r_i}\};\{\boldsymbol{R_i}\}) = V(\{\boldsymbol{R_I}\})\phi(\{\boldsymbol{r_i}\};\{\boldsymbol{R_i}\}) \tag{2.16}$$

where

$$H_e = -\sum_I \frac{\hbar^2}{2M_e}\vec{\nabla}^2_{r_i} + \frac{1}{2}\sum_{I,J}\frac{Z_I Z_J e^2}{|\boldsymbol{R_I} - \boldsymbol{R_J}|} + \frac{1}{2}\sum_{i,j}\frac{e^2}{|\boldsymbol{r_i} - \boldsymbol{r_j}|} - \sum_{I,i}\frac{Z_I e^2}{|\boldsymbol{R_I} - \boldsymbol{r_i}|} \tag{2.17}$$

and

$$[-\sum_I \frac{\hbar^2}{2M_I}\vec{\nabla}^2_{\boldsymbol{R_I}} + V(\{\boldsymbol{R_I}\})]\Theta(\{\boldsymbol{R_I}\}) = \acute{E}\Theta(\{\boldsymbol{R_i}\}) \tag{2.18}$$

Eq.(16) is the equation for the electronic problem with the nuclei positions fixed. The eigenvalue of the energy V (RI) depends on the positions of the nuclei. After solving Eq. (22), $V(\boldsymbol{R_I})$ is known and by applying it to Eq. (18), which has no electronic degrees of freedom, the motion of the nuclei is to obtained.

The significance of the BO approximation is to separate the movement of electrons and nuclei. The electrons are moving in a static external potential $V_{ext}(r)$ formed by the nuclei, which is the starting point of DFT. The BO approximation was extended by Bohn and Huang known as Born-Huang (BH) approximation [39] to take into account more nonadiabatic effect in the electronic Hamiltonian than in the BO approximation.

2.5 The Hartee Fork Approach

The Hartree–Fock (HF) method is a method of approximation for the determination of the wave function and the energy of a quantum many-body system in a stationary state.

The Hartree–Fock method often assumes that the exact N-body wave function of the system can be approximated by a single Slater determinant (in the case where the particles are fermions) or by a single permanent (in the case of bosons) of N spin-orbitals. By invoking the variational method, one can derive a set of N-coupled equations for the N spin orbitals. A solution of these equations yields the Hartree–Fock wave function and energy of the system. Especially in the older literature, the Hartree–Fock method is also called the self-consistent field method (SCF). In deriving what is now called the Hartree equation as an approximate solution of the Schrödinger equation, Hartree required the final field as computed from the charge distribution to be "self-consistent" with the assumed initial field. Thus, self-consistency was a requirement of the solution. The solutions to the non-linear Hartree–Fock equations also behave as if each particle is subjected to the mean field created by all other particles (see the Fock operator below), and hence the terminology continued.

In order to find a suitable strategy to approximate the analytically not accessible solutions of many-body problems, a very useful tool is variational calculus, similar to the least-action principle of classical mechanics. By the use of variational calculus, the ground state wave function ψ_0 , which corresponds to the lowest energy of the system E_0, can be approached. Hence, for now only the electronic Schrödinger equation is of interest, therefore in the following sections we set $\bar{H} \equiv \bar{H}_e l, E \equiv \bar{E}_e l$, and so on. Observables in quantum mechanics are calculated as the expectation values of operators. The energy as observable corresponds to the Hamil- ton operator, therefore the energy corresponding to a general Hamiltonian can be calculated as

$$E = \left\langle \bar{H} \right\rangle = \int d\vec{r_1} \int d\vec{r_2} ... \int d\vec{r_N} \psi^*(\vec{r_1}, \vec{r_2}, .., \vec{r_N}) \hat{H} \psi^(\vec{r_1}, \vec{r_2}, .., \vec{r_N}) \tag{2.19}$$

The Hatree-Fock techique is based on the principle that the energy obtained by any (normalized) trial wave function other than the actual ground state wave function is always an upper bound, i.e. higher than the actual ground state energy. If the trial function happens to be the desired ground state wave function, the energies are equal

$$E_{trial} \geq E_0 \tag{2.20}$$

with

$$E_{trial} = \int d\vec{r_1} \int d\vec{r_2} ... \int d\vec{r_N} \psi^*_{trial}(\vec{r_1}, \vec{r_2}, .., \vec{r_N}) \hat{H} \psi_{trial}(\vec{r_1}, \vec{r_2}, .., \vec{r_N}) \tag{2.21}$$

and

$$E_0 = \int d\vec{r_1} \int d\vec{r_2} ... \int d\vec{r_N} \psi^*_0(\vec{r_1}, \vec{r_2}, .., \vec{r_N}) \hat{H} \psi_0(\vec{r_1}, \vec{r_2}, .., \vec{r_N}) \tag{2.22}$$

The expressions above are usually inconvenient to handle. For the sake of a compact notation, in the following the bra-ket notation of Dirac is introduced [40]. In this notation, equations 20 to 22 are expressed as

$$\langle \psi_{trial} | \hat{H} | \psi_{trial} \rangle = E_{trial} \geq E_0 = \langle \psi_0 | \hat{H} | \psi_0 \rangle \tag{2.23}$$

Proof: The eigenfunctions ψ of the Hamiltonian $\bar{H}$ (each corresponding to an energy eigenvalue E_i) form a complete basis set, therefore any normalized trial wave function ψ trial can be expressed as linear combination of those eigenfunctions

$$\psi_{trial} = \sum_i \lambda_i \psi_i \tag{2.24}$$

The assumption is made that the eigenfunctions are orthogonal and normalized. Hence it is requested that the trial wave function is normalized, it follows that

$$\langle \psi_{trial} | \psi_{trial} \rangle = 1 = \langle \sum_i \lambda_i \psi_i | \sum_j \lambda_j \psi_j \rangle = \sum_i \sum_j \lambda^*_i \lambda_j \langle \psi_i | \psi_j \rangle = \sum_j |\lambda_j|^2 \tag{2.25}$$

On the other hand,

$$E_{trail} = \langle \psi_{trail} | \hat{H} | \psi_{trail} \rangle = \langle \sum_i \lambda_i \psi_i | \hat{H} | \sum_j \lambda_j \psi_j \rangle = \sum_j E_j |\lambda_j|^2 \tag{2.26}$$

Together with the fact that the ground state energy E_0 is per definition the lowest possible energy, and therefore has the smallest eigenvalue ($E_0 \leq E_i$), it is found that

$$E_{trail} = \sum_j E_j |\lambda_j|^2 \geq E_j \sum_j |\lambda_j|^2 \tag{2.27}$$

what resembles equation 23. Equations (19) to (27) also include that a search for the minimal energy value while applied on all allowed N-electron wave-functions will always provide the ground-state wave function (or wave functions, in case of a degenerate ground state where more than one wave function provides the minimum energy). The mathematical framework used above, i.e.rules which assign numerical values to functions, so called functionals, is also one of the main concepts in density functional theory. A function gets a numerical input and generates a numerical output whereas a functional gets a function as input and generates a numerical output. Expressed in terms of functional calculus, where $\psi \rightarrow$N addresses all allowed N-electron wave functions, this means [41]

$$E_0 = \min_{\psi \to N} E\langle \psi \rangle = \min_{\psi \to N} \langle \psi | \hat{H} | \psi \rangle = \min_{\psi \to N} \langle \psi | \hat{T} + \hat{V} + \hat{U} | \psi \rangle \tag{2.28}$$

Due to the vast number of alternative wave functions on the one hand and processing power and time constraints on the other, this search is essentially unfeasible for N-electron systems. Restriction of the search to a smaller subset of potential wave functions, as in the Hartree- Fock approximation, is conceivable.

2.6 Limitations and Failings of the Hartree-Fock Approach

The number of electrons in atoms and molecules can be even or odd. When there are even numbers of electrons and they are all positioned in double-occupied spatial orbitals ψ_i, the compound is said to be in a single state.Such systems are called closed-shell systems. Both substances with one occupied orbital, or species with a triplet or higher ground state, and substances with an odd number of electrons are referred to be open-shell systems. These two categories of systems relate to two different Hartree-Fock technique methods. All electrons are assumed to be coupled in orbitals when using the restricted HF technique (RHF), however this restriction is completely eliminated when using the unconstrained HF method (UHF). It is also possible to describe open-shell systems with a RHF approach where only the single occupied orbitals are excluded which is then called a restricted open-shell HF (ROHF) which is an approach closer to reality but also more complex and therefore less popular than UHF [42]. The size of the investigated system can also be a limiting factor for calculations. Kohn states a number of M = p^5 with 3p10 parameters for a result with sufficient accuracy in the investigation of the H_2 system [43].

For a system with N = 100 (active) electrons the number of parameters rises to

$$M = p^{3N} = 3^{300} to 10^{300} \approx 10^{150} to 10^{300} \tag{2.29}$$

The energy determined by HF calculations is usually greater than the precise ground state energy because a multi electron wave function cannot be completely represented by a single Slater determinant. The Hartree-Fock limit is the energy that can be measured with the greatest accuracy using HF techniques. The energy determined by HF calculations is usually greater than the precise ground state energy because a multi electron wave function cannot be completely represented by a single Slater determinant. The Hartree-Fock limit is the energy that can be measured with the greatest accuracy using HF methods. The difference between E_{HF} and E_{exact} is

called correlation energy and can be denoted as [44]

$$E_{corr}^{HF} = E_{min} - E_{HF} \tag{2.30}$$

Despite the fact that Ecorr is usually small against E_{min} , as in the example of a N_2 molecule where

$$\mathrm{E}_{corr}^{HF} = 14.9eV < 0.001E_{min} \tag{2.31}$$

it can have a huge influence [45].
For instance, the experimental dissociation energy of the N_2 molecule is

$$\mathrm{E}_{diss} = 9.9eV < E_{corr} \tag{2.32}$$

which corresponds to a large contribution of the correlation energy to relative energies such as reaction energies which are of particular interest in quantum chemistry. The main contribution to the correlation energy arises from the mean field approximation used in the HF-method. That means one electron moves in the average field of the other ones, an approach which completely neglects the intrinsic correlation of the electron movements. To get a better understanding what that means, one may picture the repulsion of electrons at small distances which clearly cannot be covered by a mean-field approach like the Hartree-Fock-method [46].

2.7 Slater Determination

A Slater determinant is an expression that describes the wave function of a multi-fermionic system. It satisfies anti-symmetry requirements, and consequently the Pauli principle, by changing sign upon exchange of two electrons (or other fermions). Only a small fraction of all potential fermionic wave functions can be expressed as a single slater determinant, but because of their simplicity, they are an important and useful subset. In the Hartree-Fock approach, the search is restricted to approximations of the N-electron wave function by an antisymmetric product of N (normalized) one electron wave-functions, the so called spin- orbitals $\chi_i(\vec{x_i})$ A wave function of this type is called Slater-determinant, and reads [47]

$$\Psi_0 \approx \phi_{SD} = (N!)^{-1/2} \begin{vmatrix} X_1(\vec{x_1}) & X_2(\vec{x_1}) & ... & X_N(\vec{x_1}) \\ X_1(\vec{x_2}) & X_2(\vec{x_2}) & .... & X_N(\vec{x_2}) \\ \vdots & \vdots & \vdots & \vdots \\ X_1(\vec{x_N}) & X_2(\vec{x_N}) & .... & X_N(\vec{x_N}) \end{vmatrix} \tag{2.33}$$

It is important to notice that the spin-orbitals $\chi_i(\vec{x_i})$ are not only depending on spatial co- ordinates but also on a spin coordinate which is introduced by a spin function, $\vec{x_i} = \vec{r_i}$, s A detailed discussions of the spin orbitals and their (necessary) properties are omitted in this text, a detailed treatise is provided in the books by Szabo and Holthausen [48]. As spin or- bitals e.g. hydrogen-type orbitals (for atomic calculations) and linear combinations of them are used.
Returning to the variational principle and equation (2.33), the ground state energy approximated by a single slater determinant becomes

$$E_0 = \min_{\phi_{SD} \to N} E\langle \phi_{SD} \rangle = \min_{\phi_{SD} \to N} \langle \phi_{SD} | \hat{H} | \phi_{SD} \rangle = \min_{\phi_{SD} \to N} \langle \phi_{SD} | \hat{T} + \hat{V} + \hat{U} | \phi_{SD} \rangle \tag{2.34}$$

A general expression for the Hartree-Fock Energy is obtained by usage of the Slater determinant as a trial function.

$$E_{HF} = \langle \phi_{SD} | \hat{H} | \phi_{SD} \rangle = \langle \phi_{SD} | \hat{T} + \hat{V} + \hat{U} | \phi_{SD} \rangle \tag{2.35}$$

For the sake of brevity, a detailed derivation of the final expression for the Hartree-Fock energy is omitted. It is a straightforward calculation found for example in the Book by Schwabl [49]. The final expression for the Hartree- Fock energy contains three major parts

$$E_{HF} = \langle \phi_{SD} | \hat{H} | \phi_{SD} \rangle = \sum_{i}^{N} (i|\hat{h}|i) + \frac{1}{2} \sum_{i}^{N} \sum_{j}^{N} [(ii|jj) - (ij|ji)] \tag{2.36}$$

with

$$(i|\hat{h_i}|i) = \int X_i^*(\vec{x_i})[-\frac{1}{2}\vec{\nabla_i^2} - \sum_{k=1}^{M} \frac{Z_k}{r_{ik}}] X_i(\vec{x_i}) d\vec{x_i} \tag{2.37}$$

$$(ii|jj) = \int \int |X_i(\vec{x_i})|^2 \frac{1}{r_{IJ}} |X_j(\vec{x_j})|^2 d\vec{x_i} d\vec{x_j} \tag{2.38}$$

$$(ii|jj) = \int \int |X_i(\vec{x_i}) X_j^*(\vec{x_j}) \frac{1}{r_{ij}} X_j(\vec{x_j}) X_i^*(\vec{x_i}) d\vec{x_i} d\vec{x_j} \tag{2.39}$$

The first term corresponds to the kinetic energy and the nucleus-electron interactions, $\hat{h}$ denoting the single particle contribution of the Hamiltonian, whereas the latter two terms correspond to electron-electron interactions. They are called Coulomb and exchange integral, respectively. Examination of equations (2.36) to (2.39) furthermore reveals, that the Hartree-Fock energy can be expressed as a functional of the spin orbitals $E_{HF} = E[\chi_i\ ]$ Thus,variation of the spin orbitals leads to the minimum energy. An important point is that the spin orbitals remain orthonormal during minimization. This restriction is accomplished by the introduction of Lagrangian multipliers λ_i the resulting equations, which represent the Hartree-Fock equations. For a detailed derivation, the reader is referred to the book by Szabo and Ostlund .

Finally, one arrives at

$$\hat{f}_i X_i = \lambda_i X_i \qquad i = 1, 2, ..., N \tag{2.40}$$

with

$$\hat{f}_i = -\frac{1}{2}\vec{\nabla}_i^2 - \sum_{k=1}^{M}\frac{Z_k}{r_{ij}} + \sum_{i}^{N}[\vec{J_j}(\vec{x_i} - \vec{K_j}(\vec{x_i}] = \hat{h}_i + V^{\vec{HF}}(\imath) \tag{2.41}$$

The Fock operator for the $\imath \rightarrow$ th electron.In similarity to (2.36) to (2.39), the first two terms represent the kinetic and potential energy due to nucleus-electron interaction, collected in the core Hamiltonian $\vec{h_i}$ operators,whereas the latter terms are sums over the Coulomb operator $\vec{J_j}$ and the exchange operators $\vec{K_j}$ with the other j electrons, which form the Hartree-Fock potential $V^{\vec{HF}}$.

The two electron repulsion operator from the original Hamiltonian is exchanged by a one-electron operator $V^{\vec{HF}}$ which describes the repulsion in average.

2.8 Electron Density

Electron density or electronic density is the measure of the probability of an electron being present at an infinitesimal element of space surrounding any given point.

The electron density (for N electrons) as the basic variable of density functional theory is defined as [50]

$$n(\vec{r}) = N\sum_{s_1}\int d\vec{r_2}...\int d\vec{x_N}\psi^*(\vec{r_1},\vec{x_2},...,\vec{x_N})\psi(\vec{r_1},\vec{x_2},...,\vec{x_N}) \tag{2.42}$$

If additionally the spin coordinates are neglected, the electron density can even be expressed as measurable observable only dependent on spatial coordinates [51]

$$n(\vec{r}) = N\int d\vec{r_2}...\int d\vec{r_N}\psi^*(\vec{r_1},\vec{x_2},...,\vec{x_N})\psi(\vec{r_1},\vec{x_2},...,\vec{x_N}) \tag{2.43}$$

which can e.g. be measured by X-ray diffraction. Before presenting an approach using the electron density as variable, it has to be ensured that it truly contains all necessary informations about the system. In detail that means it has to contain information about the electron number N as well as the external potential characterized by $\vec{V}$. The total number of electrons can be obtained by integration the

electron density over the spatial variables

$$N = \int d\vec{r} n(\vec{r}) \tag{2.44}$$

2.9 Thomas-Fermi-Dirac Approximation

In 1927, the predecessor to DFT was the Thomas-Fermi (TF) model proposed by Thomas [52] and Fermi [53]. They used the electron density $n(\boldsymbol{r})$ as the basic variable instead of the wavefunction. The total energy of a system in an external potential $V_{ext}(\boldsymbol{r})$ is written as a functional of the electron density $V_{ext}(\boldsymbol{r})$ as:

$$E_{TF}[n(\boldsymbol{r})] = A_1 \int n(\boldsymbol{r})^{\frac{5}{3}} d\boldsymbol{r} + \int n(\boldsymbol{r}) V_{ext}(\boldsymbol{r}) d\boldsymbol{r} + \frac{1}{2} \int \int \frac{n(\boldsymbol{r}) n(\acute{\boldsymbol{r}})}{|\boldsymbol{r} - \acute{\boldsymbol{r}}|} d\boldsymbol{r} d\acute{\boldsymbol{r}} \tag{2.45}$$

where the first term is the kinetic energy of the non-interacting electrons in a homogeneous electron gas (HEG) with $A_1 = \frac{3}{10}(3\pi^2)^{\frac{2}{3}}$ in atomic units. The kinetic energy density of a HEG is obtained by adding up all of the free electron energy state $\epsilon_k = \frac{k^2}{2}$ up to the Fermi wavevector $k_F = [3\pi^2 n(\boldsymbol{r})]^{\frac{1}{3}}$ as:

$$t_0[n(\boldsymbol{r})] = \frac{2}{(2\pi)^3} \int_0^{k_F} \frac{k^2}{2} 4\pi k^2 dk = A_1 n(\boldsymbol{r})^{\frac{5}{3}} \tag{2.46}$$

The second term is the classical electrostatic energy of the nucleus-electron Coulomb interaction. The third term is the classical electrostatic Hartree energy approximated by the classical Coulomb repulsion between electrons. In the original TF method, the exchange and correlation among electron was neglected. In 1930, Dirac [54] extended the Thomas-Fermi method by adding a local exchange term $A_2 \int n(\boldsymbol{r})^{\frac{5}{3}} d\boldsymbol{r}$ to eq. (2.41) with $A_2 = -\frac{3}{4}(\frac{3}{\pi})^{\frac{1}{3}}$ which leads eq. (2.41) to

$$E_{TFD}[n(\boldsymbol{r}] = A_1 \int n(\boldsymbol{r})^{\frac{5}{3}} d\boldsymbol{r} + \int n(\boldsymbol{r}) V_{ext}(\boldsymbol{r}) d\boldsymbol{r} + \frac{1}{2} \int \int \frac{n(\boldsymbol{r}) n(\acute{\boldsymbol{r}})}{|\boldsymbol{r} - \boldsymbol{r}'|} d\boldsymbol{r} d\acute{\boldsymbol{r}} + A_2 \int n(\boldsymbol{r})^{\frac{4}{3}} d\boldsymbol{r} \tag{2.47}$$

The ground state density and energy can be obtained by minimizing the Thomas-Fermi-Dirac equation (2.47) subject to conservation of the total number (N) of electrons. By using the technique of Lagrange multipliers, the solution can be found in the stationary condition

$$\delta\{E_{TFD}[n(\boldsymbol{r})] - \mu(\int n(\boldsymbol{r})d\boldsymbol{r} - N)\} = 0 \tag{2.48}$$

where μ is a constant known as a Lagrange multipliers, whose physical meaning is the chemical potential (or Fermi energy at T = 0 K). Eq. (2.47) leads to the Thomas-Fermi-Dirac equation.

$$\frac{5}{4}A_1 n(\boldsymbol{r})^{\frac{2}{3}} + V_{ext}(r) + \int \frac{n(\boldsymbol{r})}{|\boldsymbol{r} - \boldsymbol{r}'|}d\boldsymbol{r} = \frac{4}{3}A_2 n(\boldsymbol{r})^{\frac{1}{3}} - \mu = 0 \tag{2.49}$$

which can be solved directly to obtain the ground state density.

Chapter 3

Density Functional Theory (DFT)

Density Functional Theory (DFT) is a computational quantum mechanical modelling method used in physics, chemistry and materials science to investigate the electronic structure (or nuclear structure) (principally the ground state) of many-body systems, in particular atoms, molecules, and the condensed phases. Using this theory, the properties of a many-electron system can be determined by using functionals, i.e. functions of another function. In the case of DFT, these are functionals of the spatially dependent electron density. DFT is among the most popular and versatile methods available in condensed-matter physics, computational physics, and computational chemistry.

The electronic structure or nuclear structure, primarily the ground state of many-body systems, such as atoms and molecules, is investigated using density functional theory, a computational quantum mechanical modelling approach. It is utilized in a variety of scientific fields to obtain information about the electronic structure of several body systems, including atoms and molecules. The theory uses functional notation to describe the features of a many-electron system. The properties of a many-electron system can be determined using this theory and functionals.
The Schrödinger equation, which determines the wave-function of quantum mechanical systems, was proposed by Erwin Schrodinger in 1925 [55]. Most commonly we

deal with non-relativistic time independent Schrödinger equation :

$$H\psi = E\psi \tag{3.1}$$

Where H is the Hamiltonian operator, ψ is the eigen-function, and E is the eigen-value. The hamiltonian contain the information of kinetic and potential energy for all particles of the system. There are well known example like particle in a box or simple harmonic oscillator where the Hamiltonian has a simple form and the Schrödinger equation can be solved exactly. However, system with large number of molecule is complicated. For example, a Hamiltonian operator for a system consisting of consisting of N_i number of atoms of species i with atomic number Z_i and n species of atoms : [56]

$$\begin{aligned} H = -\frac{\hbar^2}{2}\sum_i \frac{\nabla^2_{\vec{R_i}}}{M_i} - \frac{\hbar^2}{2}\sum_i \frac{\nabla^2_{\vec{r_i}}}{m_e} - \frac{1}{4\pi\epsilon_0}\sum_{i,j}\frac{e^2 Z_i}{|\vec{R_i} - \vec{r_j}|} + \frac{1}{8\pi\epsilon_0}\sum_{i\neq j}\frac{e^2}{|\vec{r_i} - \vec{r_j}|} \\ + \frac{1}{8\pi\epsilon_0}\sum_{i\neq j}\frac{e^2 Z_i Z_j}{|\vec{R_i} - \vec{R_j}|} \end{aligned} \tag{3.2}$$

In this equation R_i and M_i are the position and mass of nuclei i respectively, and r_i and m_e are position and mass of electron i respectively. The first two terms of the right hand side describe the kinetic energy of nuclei and electrons. The next three terms describe the potential energy of the system. This potential energy arising from the attraction between electron-nucleus, electron-electron, nucleus-nucleus interaction.The hamiltonian contains kinetic and potential energy information for all particles in the system. There are well-known examples, such as the particle in a box or the simple harmonic oscillator, in which the Hamiltonian has a simple form and the Schrödinger equation may be solved precisely. However, a system with a huge number of molecules is more difficult to understand. In other word :

1. From the perspective of electron, nuclei position are static.
2. From the perspective of nuclei, electron's position are update instantaneously.

As a result, the equation (3.1) can be simplified by splitting it into two parts, an electronic and nuclear part, which can be solved separately. This kind of separation is known as Born-Oppenheimer approximation. On the Born-Oppenheimer approx-

imation, the position of the nuclei is fixed but the position of electron is not. As a result the kinetic energy term for nuclei in equation (3.1) become zero and nuclear nuclear interaction does not change.

The electronic part of the hamiltonian :

$$H_{ele} = -\frac{\hbar^2}{2}\sum_i \frac{\nabla^2_{\vec{r_i}}}{m_e} - \frac{1}{4\pi\epsilon_0}\sum_{i,j}\frac{e^2 Z_i}{|\vec{R_i} - \vec{r_j}|} + \frac{1}{8\pi\epsilon_0}\sum_{i\neq j}\frac{e^2}{|\vec{r_i} - \vec{r_j}|} \tag{3.3}$$

And it can be seen that the molecular system we are interested in can be described almost entirely by this electronic Hamiltonian. The solution of the Schrödinger equation with electronic Hamiltonian is electronic wave function ψ_{ele} with eigenvalue E_{ele}. The wave-function is a function of position only. However, it is not trivial to find ψ_{ele}. Due to the electron-electron interaction, terms in H_{ele} will be tricky to solve. Because each electron simultaneously experience an electronic repulsion though the presence of every other electron. As a result, scientists needed to come up with an approximation for wave function that will give physically sound result.

In developing this approximation, it is worth to remember that the wave-function itself can not be directly observed. Instead what we can be measured is the probability that N electrons at some particular set of position $(\vec{r_1}, ..., \vec{r_N})$. The probability is given by :

$$|\psi(\vec{r_1}, ..., \vec{r_N})|^2 = \psi^*(\vec{r_1}, ..., \vec{r_N})\psi(\vec{r_1}, ..., \vec{r_N}) \tag{3.4}$$

$\psi(\vec{r_1}, ..., \vec{r_N})$ can be approximated as a product of individual wave functions which is known as "Hatree product". Also we need to remember that all electron are identical. So we can not level them as electron 1 or electron N, but we can measure the probability that any order of set of N electrons are in the coordinate $\vec{r_1}$ to $\vec{r_n}$. So the electron density can be calculated like:

$$n(\vec{r}) = 2\sum_i \psi_i^*(\vec{r})\psi_i(\vec{r}) \tag{3.5}$$

The factor 2 come because of electron spin. The electron density is a factor of three

coordinate, but can give a lot of information that is observable from wave-function which is a function of 3N coordinate.
Walter Kohn with his co-workers developed the "Density functional theory" to find how to use the electron density for the solution of Schrödinger equation and for his work, he got novel prize in 1998 [57].

3.1 Hohenberg-Kohn Theorems

In 1964, DFT was proven to be an exact theory of many-body systems by Hohenberg and Khon. [58] It applies to condensed-matter systems of electrons with fixed nuclei, and also to any system of interacting particles in an external potential $V_{ext}(\vec{r})$. The theory is based upon two theorems.

The HK Theorem I

The ground state particle density $n(\boldsymbol{r})$ of a system of interacting particle in an external potential $V_{ext}(\vec{r})$ uniquely determines the external potential $V_{ext}(\vec{r})$, except for a constant. Thus the ground state particle density determines the full hamiltonian, except for a constant shift of the energy. In principle, all the states including ground and excited states of many-body wavefunctions can be calculated. This means that the ground state particle density uniquely determines all properties of the system completely.
Proof: For simplicity, consider the case that the ground state of the system is nondegener- ate. It can be proven that the theorem is valid for systems with degenerate ground states [59]. The proof is based on minimum energy principle. Suppose there are two different external potentials $V_{ext}(\vec{r})$ and $V_{ext}(\vec{r})$ which differ by more than a constant and lead to the same ground state density $n_0(\boldsymbol{r})$. The two external potentials would give two different Hamiltonians, $\hat{H}$ and $\acute{\hat{H}}$, which have the same ground state density $n_0(\boldsymbol{r})$ but would have different ground state wavefunctions, Ψ and $\acute{\Psi}$, with $\hat{H} = E_0\psi$ and $\hat{H} = \acute{E}_0\acute{\psi}$. Since $\acute{\psi}$ is not the ground state of $\hat{H}$, it

follows that

$$E_0 < \langle \Psi' | \hat{H} | \Psi' \rangle < \langle \Psi' | \hat{H}' | \Psi' \rangle + \langle \Psi' | \hat{H} - \hat{H}' | \Psi' \rangle < E_0' + \int n_0(\boldsymbol{r})[V_{ext} - V_{ext}'(\boldsymbol{r})]d\boldsymbol{r} \tag{3.6}$$

Similarly

$$E_0' < \langle \Psi | \hat{H} | \Psi \rangle < \langle \Psi | \hat{H} | \Psi \rangle + \langle \Psi | \hat{H} - \hat{H} | \Psi \rangle < E_0 + \int n_0(\boldsymbol{r})[V_{ext}' - V_{ext}(\boldsymbol{r})]d\boldsymbol{r} \tag{3.7}$$

Adding eq. (63) and (64) lead to the contradiction

$$E_0 + E_0' < E_0 + E_0' \tag{3.8}$$

Hence, the ground state density determines the external potential $V_{ext}(\vec{r})$, except for a constant. There is one-to-one mapping between the ground state density $n_0(\boldsymbol{r})$ and the external potential $V_{ext}(\vec{r})$, although the exact formula is unknown.

The HK Theorem II

There exists a universal functional $F[n(\boldsymbol{r})]$ of the density, independent of the external potential$V_{ext}(\vec{r})$, such that the global minimum value of the energy functional$E[\Psi'] \equiv \int n(\boldsymbol{r})V_{ext}(\boldsymbol{r})d\boldsymbol{r} + F[n(\boldsymbol{r})]$ is the exact ground state energy of the system and the exact ground state density $n_0(\boldsymbol{r})$ minimizes this functional. Thus the exact ground state energy and density are fully determined by the functional $E[\Psi']$.

Proof:

The universal functional $F[n(\boldsymbol{r})]$ can be written as

$$F[n(\boldsymbol{r})] \equiv T[n(\boldsymbol{r})] + E_{int}[n(\boldsymbol{r}] \tag{3.9}$$

where $T[n(\boldsymbol{r})]$ is the kinetic energy and $E_{int}[n(\boldsymbol{r})]$ is the interaction energy of the particles. According to variational principle, for any wavefunction Ψ' , the energy functional$E[\Psi']$:

$$E[\Psi'] \equiv \langle \Psi' | \hat{T} | \hat{V_{int}} + \hat{V_{ext}} | \Psi' \tag{3.10}$$

has its global minimum value only when Ψ' is the ground state wavefunction ψ_0 with the constraint that the total number of the particle is conserved. According to HK theorem I, Ψ' must correspond to a ground state with particle density $n'(\boldsymbol{r})$ and external potential $V_extt'(\boldsymbol{r})$, then $E[\Psi']$ is a functional of $n'(\boldsymbol{r})$. According to variational principle:

$$\begin{aligned} E[\Psi'] \equiv \left\langle \Psi' | \hat{T} + \hat{V_{int}} + \hat{V_{ext}} | \Psi' \right. &= E[n'(\boldsymbol{r})] \\ &= \int n'(\boldsymbol{r}) V'_{ext}(\boldsymbol{r}) d\boldsymbol{r} + F[n'(\boldsymbol{r})] \\ &> E[\Psi_0] \\ &= \int n_0(\boldsymbol{r}) V_{ext}(\boldsymbol{r}) d\boldsymbol{r} + F[n_0(\boldsymbol{r})] \\ &= E[n_0(\boldsymbol{r}] \end{aligned} \tag{3.11}$$

Thus the energy functional $E[\Psi'] \equiv \int n(\boldsymbol{r}) V_{ext}(\boldsymbol{r}) d\boldsymbol{r} + F[n(\boldsymbol{r})]$ evaluated for the correct ground state density $n_0(\boldsymbol{r})$ is indeed lower than the value of this functional for any other density $n(\boldsymbol{r})$. Therefore by minimizing the total energy functional of the system with respect to variations in the density $n(\boldsymbol{r})$, one would find the exact ground state density and energy.

3.2 Kohn-Sham Formulation

Kohn and Sham proposed a method to solve equation (8) [60] based on two approximations described as follows [61]: 1. The ground state density is equivalent to the ground state of collection of non-interacting particles in an auxiliary system.
2. The Hamiltonian for the auxiliary system is constructed with the normal kinetic energy operator,but the auxiliary potential is treated as an effective local potential. This approximation best work for densities which are smooth and varying slowly.

The framework by Hohenberg and Kohn is exact, yet not very useful in actual calculations. The only possibility would be the direct use of the second Hohenberg-Kohn

theorem for energy minimization, a way that is possible in general but has proven itself to be impractical [62].

The Hartree-equations are clearly wave-function based and not directly related to the work of Hohnberg and Kohn, yet they have been proven very useful. Hartree's approximation assumes that every electron moves in an effective single-particle potential of the form

$$\upsilon_H(\vec{r}) = -\frac{Z}{|\vec{r}|} + \int \frac{n(\vec{r'})}{|\vec{r} - \vec{r'}|} d\vec{r} \tag{3.12}$$

The first term is an attractive Coulomb potential of a nucleus with atomic number Z, whereas the integral term corresponds to the potential caused by the mean electron density distribution $n(\vec{r})$.

The mean density can be denoted in terms of the single particle wave functions

$$n(\vec{r}) = \sum_{j=1}^{M} |\phi_j(\vec{r})|^2 \tag{3.13}$$

Since the electron-electron interactions are taken into account in the potential term, the N-electron and therefore (neglecting the spin coordinates) 3N-dimensional Schrdinger equation can be approximately replaced by N 3-dimensional single particle equations for electrons moving in an effective potential defined in (3.13):

$$[-\frac{1}{2}\vec{\nabla}^2 + \upsilon_H(\vec{r})]\psi_j(\vec{r}) = \epsilon_j \psi_j(\vec{r}) \tag{3.14}$$

Therefore, Kohn and Sham investigated the density functional theory applied to a system of N non-interacting electrons in an external potential, similar to Hartree's approach. The expression for the energy of such a system is of the form

$$E_{\upsilon(\vec{r})}[n'(\vec{r})] = \int \upsilon(\vec{r}) n'(\vec{r}) d\vec{r} + d\vec{r} + T_S[n'(\vec{r})] \geq E \tag{3.15}$$

where $n'(\vec{r'})$ is a υ-representable density for non-interacting electrons and $T_S[n'(\vec{r})]$ the kinetic energy of the ground state of those non-interacting electrons.

Setup of the Euler-Lagrange equation [63] for the non-interacting case with the

density defined in (3.15) as argument provides

$$\delta E_{\upsilon} \equiv \int \delta n'(\vec{r})[\upsilon(\vec{r}) + \frac{\delta}{\delta n'(\vec{r})} T_S[n'(\vec{r})]|_{n'(\vec{r})=n(\vec{r})} - \epsilon] d\vec{r} = 0 \tag{3.16}$$

For a system of non-interacting electrons, the total ground state energy and particle density can therefore simply be denoted as the sums

$$E = \sum_{j=1}^{N} \epsilon_j \tag{3.17}$$

and

$$n(\vec{r}) = \sum_{j=1}^{N} |\phi_j(\vec{r})|^2 \tag{3.18}$$

In addition, Kohn and Sham used the universal functional as an alternative formulation,

$$F[n'(\vec{r})] \equiv T_S[n'(\vec{r})] + \frac{1}{2} \int \frac{[n'(\vec{r})][n'(\vec{r'})]}{|\vec{r} - \vec{r'}|} d\vec{r} d\vec{r'} + E_{xc}[n'(\vec{r})] \tag{3.19}$$

In (3.19) $T_S[n'(\vec{r})]$ is the kinetic energy functional of non-interacting electrons (which is not even for the same density $n(\vec{r})$ the true kinetic energy of the inter- acting system) and the second term is the so-called Hartree term which describes the electrostatic self-repulsion of the electron density [64]. The last term is called exchange-correlation term. It is implicitly defined by (3.19) and can in practice only be approximated. The quality of the approximation for $E_{xc}[n'(\vec{r})]$ is therefore one of the key issues in DFT.

Construction of the Euler-Lagrange equations for the interacting case in equation (3.19) provides

$$\delta E_{\upsilon} \equiv \int \upsilon n'(\vec{r})[\upsilon_{eff}(\vec{r}) + \frac{\delta}{\delta n'(\vec{r})} T_S[n'(\vec{r})]|_{n'(\vec{r})=n(\vec{r})} - \epsilon] d\vec{r} = 0 \tag{3.20}$$

with

$$\upsilon_{eff}(\vec{r}) \equiv \upsilon(\vec{r}) + \int \frac{[n(\vec{r})]}{|\vec{r} - \vec{r'}|} d\vec{r} + \upsilon_{xc}(\vec{r} \tag{3.21}$$

and the functional derivative

$$\upsilon_{xc}(\vec{r}) \equiv \frac{\delta}{\delta n'(\vec{r})} E_{xc}[n'(\vec{r})]|_{n'(\vec{r})=n(\vec{r})} \tag{3.22}$$

whereas the Euler-Lagrange equation resembles (3.19) up to the potential term. Because of that, the minimizing density can be calculated in a way similar to the Hartree- approach described in equations (3.20) to (3.23). The corresponding equations are the single-particle Schrödinger equations

$$[-\frac{1}{2}\vec{\nabla}^2 + \upsilon_{eff}(\vec{r}) = \epsilon_j \psi_j(\vec{r}) j = 1, 2, ..., N \tag{3.23}$$

as well as the defining equation for the particle density

$$n(\vec{r}) = \sum_{j=1}^{M} |\psi_j(\vec{r})|^2 \tag{3.24}$$

which form together with the effective potential$\upsilon_{eff}(\vec{r})$ in (3.25) the self-consistent Kohn-Sham equations.

The accurate ground state energy, as one of the most important quantities, can be expressed as

$$E = \sum_j \epsilon_j + E_{xc}[n(\vec{r})] - \int \upsilon_{xc}(\vec{r}) n(\vec{r}) d\upsilon - \frac{1}{2} \int \frac{[n'(\vec{r})][n'(\vec{r'})]}{|\vec{r} - \vec{r'}|} d\vec{r} d\vec{r'} \tag{3.25}$$

Equation (3.25) can be seen as an generalization of the energy expression obtained with the Hartree-approach (note that the neglect of $E_{xc}[n(\vec{r})]$ and $\upsilon_{xc}(\vec{r})n(\vec{r})$ leads back to equation (3.24)).

3.3 Solving the Kohn-Sham equations

Once we have approximated the exchange-correlation energy, we are in a position to solve the Kohn-Sham equations. The Kohn-Sham equations have an it-

erative solution; they have to be solved self-consistently. To solve the Kohn-Sham equations for a many body system, we need to define the Hartree potential and the exchange-correlation potential, and to define the Hartree potential and the exchange-correlation potential, we need to know the electron density n(r). By using independent-particle methods, the KS equations provide a way to obtain the exact density and energy of the ground state of a condensed matter system. The KS Given that the effective KS potential VKS and the constant KS, equations must be consistently solved. $n(r)$ and electron density are closely linked terms. This is usually done numerically through some self-consistent iterations as shown in Figure 3.1.

The process starts with an initial electron density, usually a superposition of atomic electron density, then the effective KS potential V_{KS} is calculated and the KS equation is solved with single-particle eigenvalues and wavefunctions, a new electron density is then calculated from the wavefunctions. After this, self-consistent condition(s) is checked. Self-consistent condition(s) can be the change of total energy or electron density from the previous iteration or total force acting on atoms is less than some chosen small quantity, or a combination of these individual conditions. If the self-consistency is not achieved, the calculated electron density will be mixed with electron density from previous iterations to get a new electron density. A new iteration will start with the new electron density. This process continues until self-consistency is reached. After the self-consistency is reached, various quantities can be calculated including total energy, forces, stress, eigenvalues, electron density of states, band structure, etc..

Solving the Kohn-Sham equation with a given Kohn-Sham potential VKS is the phase that takes up the most time in the entire procedure. When boundary conditions are used, there are numerous different methods for calculating the independent particle electronic states in solids. They are basically classified into three types :

1. Plane waves: In this method, the wave functions (eigenfunctions of the KS equations) are expanded in a complete set of plane waves and the external potential of nuclei are replaced by pseudopotentials which include effects from core elec-

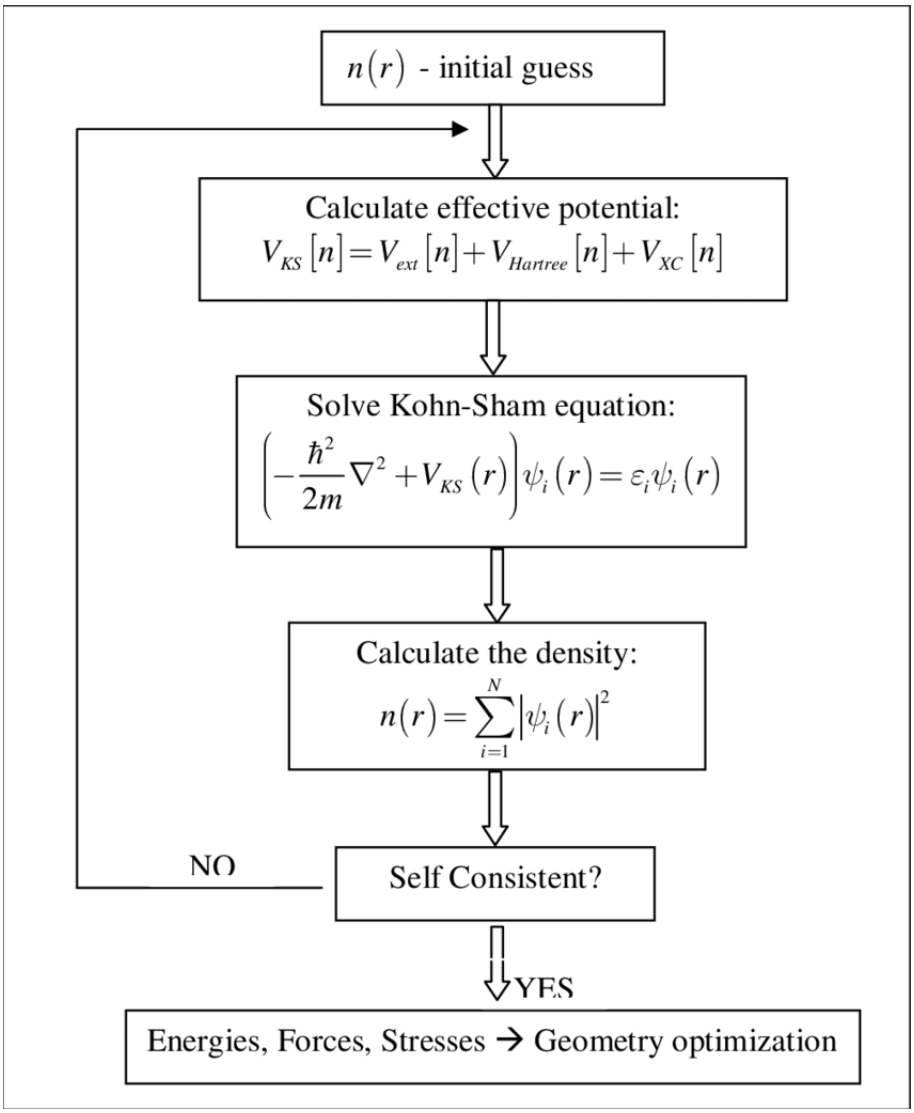

Figure 3.1: Flowchart of self-consistency loop for solving KS equations

trons. Such pseudopotentials have to satisfy certain conditions. Most widely used pseudopotentials nowadays include norm conserving pseudopotentials (NCPPs) and ultrasoft pseudopotentials (USPPs). In norm-conserving pseudopotentials, five requirements should be satisfied:

The pseudo valence eigenvalues should agree with all-electron valence eigenvalues for the chosen atomic reference configuration. The pseudo valence wavefunctions should match all- electron valence wavefunctions beyond a chosen core radius R_c. The logarithmic derivatives of the pseudo and the all-electron wavefunctions should agree at R_c. The integrated charge inside $R_c$for each wavefunction agrees (norm-conservation) and the first energy derivative of the logarithmic derivatives of the all-electron and pseudo wavefunctions agree at R_c and therefore for all $r \leq R_c$.

In ultrasoft pseudopotentials, the norm-conservation condition is not required so that the pseudo wavefunctions are much softer than pseudo wavefunctions in norm conserving pseudopotentials. As a result, it significantly reduces the number of plane waves needed to expand the wavefunctions (smaller energy cutoff for wavefunctions). Plane waves have played an important role in the early orthogonalized plane wave (OPW) calculations and are generalized to modern projector augmented wave (PAW) method. Because of the simplicity of plane waves and pseudopotentials, computational load is significantly reduced in these methods and therefore it is most suitable for calculations of large systems. In this method, forces can be easily calculated and it can be easily developed to quantum molecular dynamics simulations as well as response to (small) external perturbations. However, results from plane wave methods using pseudopotentials are usually less accurate than results from all-electron full potential methods. And great care should be taken when one generates a pseudopotential and it should be tested to match results from all-electron calculations. The most widely used codes using plane waves and pseudopotentials are plane wave self-consistent field (now known as Quantum ESPRESSO) (PWscf), ABINIT , VASP (which uses PAW method too).

2. Localized atomic orbitals: The most well-known methods in this category are linear combination of atomic orbitals (LCAO), also called tight-binding (TB) and full potential non-orthogonal local orbital (FPLO). The basic idea of these methods is to use atomic orbitals as the basis set to expand the one- electron wavefunction in KS equations.

In FPLO, in addition to the spherical average of the crystal potential, a so-called confining potential $V_{con} = (r/r_0)^m$ is used to compress the long range tail of the local orbitals (wave functions), where m is the confining potential exponent with a typical value of four, $r_0 = (x_0 r_N N/2)^{\frac{3}{2}}$ is a compression parameter with x_0 being a dimensionless parameter and rNN the nearest neighbor distance. Therefore, the atomic-like potential is written as

$$V_{at}(r) = -(\frac{1}{4\pi}) \int V(r - R - \tau) d^3r + V_{con}(r) \tag{3.26}$$

where the first term is the spherical average of the crystal potential mentioned above. For systems containing atom(s) with partially filled 4f and 5f shells, the confining potential exponent m needs to be increased to 5 or 6. In practice, the dimensionless parameter x_0 is taken as a variational parameter in the self-consistent procedure.

3. Atomic sphere Methods in the class can be considered as a combination of plane wave method and localized atomic orbitals. It uses localized atomic orbital presentation near the nuclei and plane waves in the interstitial region. The most widely used methods are (full potential) linear muffin-tin orbital (LMTO) as implemented in LMTART by Dr. Savrasov and (full potential) linear augment plane wave (LAPW) as implemented in WIEN2k.

However, to find the electron density, we must know the single electron wave functions. We do not know these wave functions until we solve the Kohn-Sham equations. The well-known approach to solve the Kohn-Sham equations is to start with an initial trial electron density as illustrated in Figure 3.1. Then solve these equations using the trial electron density. After solving the Kohn-Sham equations, we will have a set of single electron wave functions. Using these wave functions, we can calculate the new electron density. The new electron density is an input for the next cycle. Finally, compare the difference between the calculated electron densities for consecutive iterations. If the difference in electron density between consecutive iterations is lower than an appropriately chosen convergence criterion, then the solution of the Kohn-Sham equations is said to be self-consistent. Now the calculated electron density is considered as the ground state electron density, and it can be used to calculate the total energy of the system [65].

3.4 Exchange Correlation Functionals/Potentioals

Since the exchange-correlation functional's real form is unknown, solving the Khon-Sham equations presents a significant challenge. For the exchange-correlation functional, there are two basic approximation techniques that have been used. The exchange-correlation functional in DFT computations can be roughly modeled using the local density approximation (LDA).The second well known class of approxima-

tions to the Khon-Sham exchange-correlation functional is the generalized gradient approximation (GGA). In the GGA approximation the exchange and correlation energies include the local electron density and the local gradient in the electron density [66].

3.5 mBJ (modified Becke Johnson)

Spin DFT is important in the theory of atoms amd molecules with net spins, as well as solids with magnetic order. The relevent example for our purpose is the Zeeman term that is different Fermions with up and down spin. According to this model the particle density,

$$n(r) = n(r, \sigma =\uparrow) + n(r, \sigma =\downarrow) \tag{3.27}$$

and the spin density

$$s(r) = n(r, \sigma =\uparrow) - n(r, \sigma =\downarrow) \tag{3.28}$$

This results the energy density as

$$E = E_{HK}[n, s] \equiv E_{HK}^{'} \tag{3.29}$$

Where [n] denotes the functionl of the density which depends both on space and spin. In absance of external Zeeman fields, the soluton of lowest energy may be spin polarized. This is,

$$n(r, \sigma =\uparrow) \neq n(r, \sigma =\downarrow) \tag{3.30}$$

which is anologous to the broken symmetry solution of unrestricted Hartree-Fock theorem. The usefulness of spin Density Functional Theory is in these cases as well. The original Hartree-Fock theorem are valid and the ground state is determined by total ground state density $n(r, \sigma =\uparrow) + n(r, \sigma =\downarrow)$ for the system where there is no spin dependent external potential.

3.6 PBE (Perdew Burke Ernzerhof)

The PBE form is the simplest GGA (Generalized Gradient Approximation) functional. Hence we give it as an explicit example. The reader is referred to other sources such as the paper on Comparison shopping for a gradient-corrected density functional, by Perdew and Burke. The PBE functional for exchange is given by a simple form for the enhancement factor F_x.The form is chosen with $F_x(0) = 1$ (so that the local approximation is recovered) and F_x constant at large s,

$$F_x(s) = 1 + \kappa - \frac{\kappa}{(1 + \frac{\mu s^2}{\kappa})} \tag{3.31}$$

where $\kappa = 0.804$ is chosen to satisfy the LiebOxford bound. The value of $\mu = 0.21951$ is chosen to recover the linear response form of the local ap- proximation, i.e. it is chosen to cancel the term from the correlation. This may seem strange, but it is done to agree better with quantum Monte Carlo calculations. This choice violates the known expansion at low s given in Eq. (3.31), with the rationale of better fitting the entire functional. Correlation takes the form of a local correlation and an additive term, both of which are dependent on gradients and spin polarization [67].
The form chosen to satisfy a number of requirements is

$$E_c^{GGA-PBE}[n\uparrow, n\downarrow] = \int d^3rn[\epsilon_C^{hom}(r_s, \zeta) + H(r_s, \zeta, t)] \tag{3.32}$$

where $\zeta = (n\uparrow, n\downarrow)/n$ is the spin polarization,r s is the local value of the density parameter, and t is a dimensionless gradient $t = |\nabla n|/(2\phi\kappa_{TF}n)$ .Here $\phi = ((1 + \zeta)^{\frac{2}{3}} + (1\zeta)^{\frac{2}{3}})/2$ and t is scaled by the screening wavevector k_TF rather than k_F . The final form is

$$H = \frac{e^2}{a_0}\gamma\phi^3 log(1 + \frac{\beta}{\gamma}t^2\frac{1 + At^2}{1 + At^2 + A^2t^4} \tag{3.33}$$

where the factor $\frac{e^2}{a_0}$, with a_0 the Bohr radius, is unity in atomic units. The function A is given by

$$A = \frac{\beta}{\gamma}[exp(\frac{-\epsilon_c^{hom}}{\gamma\phi^3\frac{e^2}{a_0}} - 1]^{-}1 \tag{3.34}$$

$$\prod_{\substack{k=0 \\ k\neq i}} \tag{3.35}$$

3.7 Applications

The density of states appears in many areas of physics, and helps to explain a number of quantum mechanical phenomena. Some uses of DFT are: Calculating the density of states for small structures shows that the distribution of electrons changes as dimensionality is reduced. For quantum wires, the DOS for certain energies actually becomes higher than the DOS for bulk semiconductors, and for quantum dots the electrons become quantized to certain energies [68].

LDOS can be used to gain profit into a solid-state device. For example, the figure on the right illustrates LDOS of a transistor as it turns on and off in a ballistic simulation. The LDOS has clear boundary in the source and drain, that corresponds to the location of band edge. In the channel, the DOS is increasing as gate voltage increase and potential barrier goes down [69].

An important feature of the definition of the DOS is that it can be extended to any system. One of its properties are the translationally invariability which means that the density of the states is homogeneous and it's the same at each point of the system. But this is just a particular case and the LDOS gives a wider description with a heterogeneous density of states through the system [70].

DFT is used to study other properties like optical property, magnetic property of a material. By computing the electronic band structure and density of states (DOS), DFT is utilised to comprehend a material's optical characteristics. By analyzing the band structure and DOS, it is possible to determine the electronic transitions that give rise to the material's absorption and emission spectra. Other optical characteristics, such the refractive index and the dielectric function, may be calculated

using DFT and are crucial for understanding how light interacts with the material. DFT can measure a material's magnetic moment, which indicates its magnetic field strength. They can calculate magnetic susceptibility, which measures how quickly a substance magnetises in a magnetic field. DFT also study ferromagnetism, anti-ferromagnetism, and spin glass behaviour [70].

The photon density of states can be manipulated by using periodic structures with length scales on the order of the wavelength of light. Some structures can completely inhibit the propagation of light of certain colors (energies), creating a photonic band gap: the DOS is zero for those photon energies. Other structures can inhibit the propagation of light only in certain directions to create mirrors, waveguides, and cavities. Such periodic structures are known as photonic crystals. In nanostructured media the concept of local density of states (LDOS) is often more relevant than that of DOS, as the DOS varies considerably from point to point [71].

DFT can be used to study the X-ray absorption spectra and X-ray emission spectra of a material. X-ray absorption spectroscopy (XAS) examines how the amount of X-rays absorbed by a sample changes with the energy of the X-rays. The absorption spectrum shows how the particles in the material are put together electronically. On the other hand, X-ray emission spectroscopy (XES) tracks how the energy of the light that a sample gives off after being excited by X-rays. DFT can be used to figure out how the material's electrons are organized and to model the XAS and XES spectra. By comparing the simulated spectrum to the real spectrum, you can learn about the electronic structure of the object [72].

Chapter 4

Result and Discussion

Before dealing with any double perovskites compound, it is essential to understand the compound's properties such as its electrical and optical ones. Nevertheless, the experimental technique requires a lot of resources or financial backing. Computational studies based on density functional theory can guide experimental efforts and, in many cases, offer a deeper understanding of the synthesis, related properties, and use of new materials.

Density functional theory may be used to determine many different properties, including electronic, optical, elastic, and thermoelectronic. The WIEN2k package, a computer program, investigates structural, electrical, magnetic, and optical characteristics using the full-potential linearized augmented plane wave approach (FP-LAPW) based on density functional theory (DFT) [73]. To identify the ideal ground states of the materials under study, the Perdew-Burke-Ernzerhof (PBE) approximation [74] can be employed in combination with the generalized gradient approximation (GGA). Nevertheless, since the electronic bandgap is overestimated by the PBE-GGA level of theory, it is feasible to construct more accurate band gaps using the Trans and Blaha modified Becke and Johnson potential (TB-mBJ) [75].

4.1 Method of Calculation

Under the framework of density functional theory, the structural, electronic, optical properties of the Ca_2GaAsO_6 are investigated using full potential linearized augmented plane (FP-LAPW) method, approach implemented in the WIEN2k package. The generalized gradient approximation (GGA) for determining the exchange and correlation potential energy in Khon-Sham equation that gives the final result. The generalized gradient approximation is used to optimize the parameters (RK_{max} , k-point, and lattice constant). For the double perovskitess Ca_2GaAsO_6 the RMT values taken for Ca, Ga, As, and O are 2.5, 1.93, 1.81, and 1.64 a.u. respectively. We set $RK_{max} = 7$ after optimization of energy where, R is the smallest radius of the muffin-tin sphere and RK_{max} is the largest reciprocal lattice vector that used in the expansion of flat wave function. Moreover, the number of k-point has selected to 4000 for SCF (Self Consistent Field) in Brillouin zone and 20000 for DOS calculation. The charge convergence and energy convergence has selected respectively 0.001 e and 0.00001 Ry during SCF (Self Consistent Field) cycle calculation.
The Murnaghan equation of state is used to compute energy as a function of latice constant in order to determine the stability of the compound in the structure under investigation before moving on to any electronic or magnetic properties. The volume optimization is provided with WIEN2k package that determines the minimum energy possessed by a system by plotting volume vs energy graph. It is clear that every system tries to in its minimum energy level and so we plotted total energy vs volume plots.

4.2 Structural Properties

In this thesis, the structure of double perovskites Ca_2GaAsO_6 is generated by XCryS-Den software in WIEN2k. The crystral structure with space group-225 ($Fm\bar{3}m$) for the double perovskitess Ca_2GaAsO_6 is a cubic structure. A simple structure of

double perovskites is given in Figure 4.1:

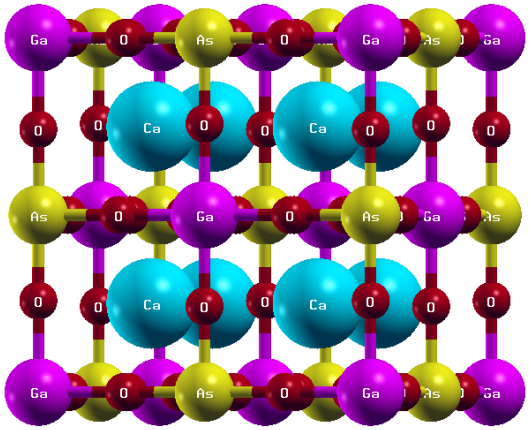

Figure 4.1: Crystal structure of the double perovskites Ca_2GaAsO_6

A unit cell of this crystal structure contains 143 atoms, 258 bonds, and 35 polyhedra.Out of the 143 atoms, Ca has 8 atoms, Ga has 14 atoms, As has 13 atoms, and O has 108 atoms.We found unit cell volume = 439.377339 $\mathring{A}$ Here, we calculated energy as a function of lattice constant in order to determine the stability of the compound in the structure under investigation before moving on to any electronic or magnetic properties. The volume optimization feature of the WIEN2k package calculates the system's smallest energy requirement by plotting the volume vs. energy graph outlined in Figure 4.2:

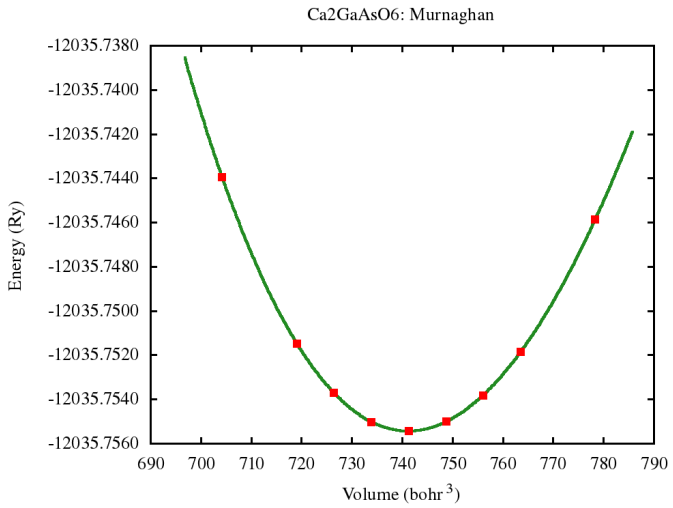

Figure 4.2: Volume optimization curve of Ca_2GaAsO_6

By volume optimization, the lattice constant has found to be 14.366300 bohr. It is clear that every system tries to in its minimum energy level, and so we plotted total energy vs volume plots. By using Murnaghan fit we see that the calculated minimum energy = -12035.75543376 Ry corresponding to the volume of 741.32915 $bohr^3$

4.3 Electronic Properties

The number of unique states that electrons can occupy at a given energy level or the number of electron states per unit volume per unit energy is known as the density of states (DOS). The bulk properties of conductive substances, such as specific heat, paramagnetic susceptibility, and other transport phenomena, are controlled by this function.

We must use generalized gradient approximation GGA, which is available as Perdew-Burke-Ernzerhof (PBE) functional, to calculate the band structure and total density of state (TDOS) in order to understand the electrical properties of double perovskites Ca_2GaAsO_6.

The optical properties of a material defines how it interacts with light. We have studied the dielectric function, reflectivity, optical conductivity, refractive index, ab-

sorption coefficient, and electron energy loss for understanding the optical properties of double perovskites Ca_2GaAsO_6 by generalized gradient approximation (GGA).

4.3.1 Band Theory and Band Gap

The introduction of band theory happened during the quantum revolution in science. Walter Heitler and Fritz London discovered the energy bands [76].
We know that the electrons in an atom are present in different energy levels. When we try to assemble a lattice of a solid with N atoms, then each level of an atom must split up into N levels in the solid. This splitting up of sharp and tightly packed energy levels forms Energy Bands. The gap between adjacent bands representing a range of energies that possess no electron is called a Band Gap.
The band gap generally refers to the energy difference between the top of the valence band and the bottom of the conduction band in insulators and semiconductors. It is the energy required to promote a valence electron bound to an atom to become a conduction electron, which is free to move within the crystal lattice and serve as a charge carrier to conduct electric current.
The distinction between semiconductors and insulators is a matter of convention. One approach is to think of semiconductors as a type of insulator with a narrow band gap. Insulators with a larger band gap, usually greater than 3 eV.

The band-gap energy of semiconductors tends to decrease with increasing temperature. When temperature increases, the amplitude of atomic vibrations increases, leading to larger interatomic spacing. The interaction between the lattice phonons and the free electrons and holes will also affect the band gap to a smaller extent. The relationship between band gap energy and temperature can be described by Varshni's empirical expression.

$$E_g(T) = E_g(m) - \frac{\alpha T^2}{T + \beta} \tag{4.1}$$

where $E_g(m)$, α and $\beta$are material constants.

4.3.2 Band Structure

The investigation of the electronic band structure is necessary to understand the physical properties of crystalline solids which almost completely describe optical as well as transport properties. One of the main goals of this thesis is to generate the band structure and determine the band gap of double perovskitess Ca_2GaAsO_6.
We used the WIEN2k software to generate the band structure. It is noticed that the band is not overlap between the conduction band and the valence band in the Fermi level both in the Figure 4.3a and 4.3b:

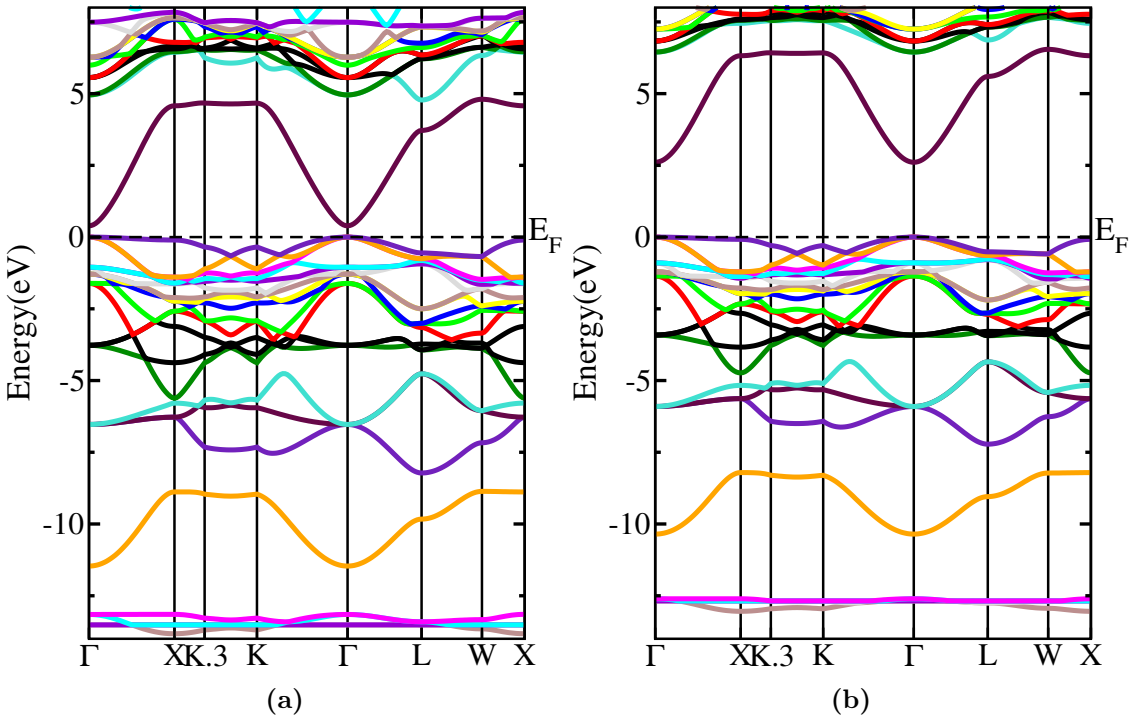

Figure 4.3: Band gap of Ca_2GaAsO_6 compound in (a)PBE and (b)mBJ

The energy gap between the top of the Valance Band (VB) and the bottom of the Conduction Band (CB) is approximately 0.393 eV for PBE potential and 2.607 eV for mBJ potential. The valance band maximum and conduction band minimum are located at the Γ point. The electronic band structure of Ca_2GaAsO_6 in Figure 4.3 shows semiconducting behavior.

4.3.3 DOS and PDOS

The number of unique states that electrons can occupy at a given energy level, or the number of electron states per unit volume per unit energy, is known as the density of states (DOS). The bulk properties of conductive substances, such as specific heat, paramagnetic susceptibility, and other transport phenomena, are controlled by this function. The density of states is directly related to the dispersion relations of the properties of the system. High DOS at a specific energy level means that many states are available for occupation. Advancements in first-principles techniques for studying the electronic structures of materials [77] have made calculations of the density of states routine [78, 79]; yet, some that are published do not exhibit the features described in this review. To calculate a sufficient-quality DOS, appropriate input parameters must be explicitly specified. Depending on the quantum mechanical system, the density of states can be calculated for electrons, photons, or phonons, and can be given as a function of either energy or the wave vector k. To convert between the DOS as a function of the energy and the DOS as a function of the wave vector, the system-specific energy dispersion relation between E and k must be known.

The density of state (DOS) of double perovskites Ca_2GaAsO_6 for PBE potential and mBJ potential is shown in the Figure 4.4 :

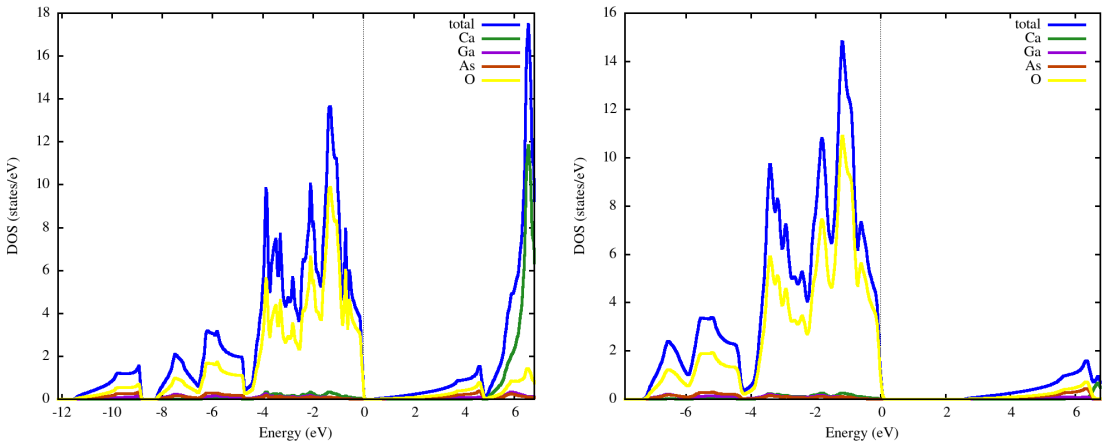

Figure 4.4: Density of State (DOS) of Ca_2GaAsO_6 compound in (a)PBE and (b)mBJ

One needs to compute the DOS of the system for detailed studies of the formation of energy bands. From previous section we got the band gap approximately 0.393 eV for PBE potential and 2.607 eV for mBJ potential which indicates the compound is semiconductor. From Figure 4.4, it is clear that the total DOS has peaks in the valence band region is slightly less than the conduction band region for PBE potential but more than for mBJ potential. It means most of the electrons in different atoms are not free from their respective atoms for mBJ potential. The contribution of electrons of O atoms in the valence band is way greater than other atoms in both potential but contribution of electrons of Ca is greater than other atoms in conduction band for PBE potential.

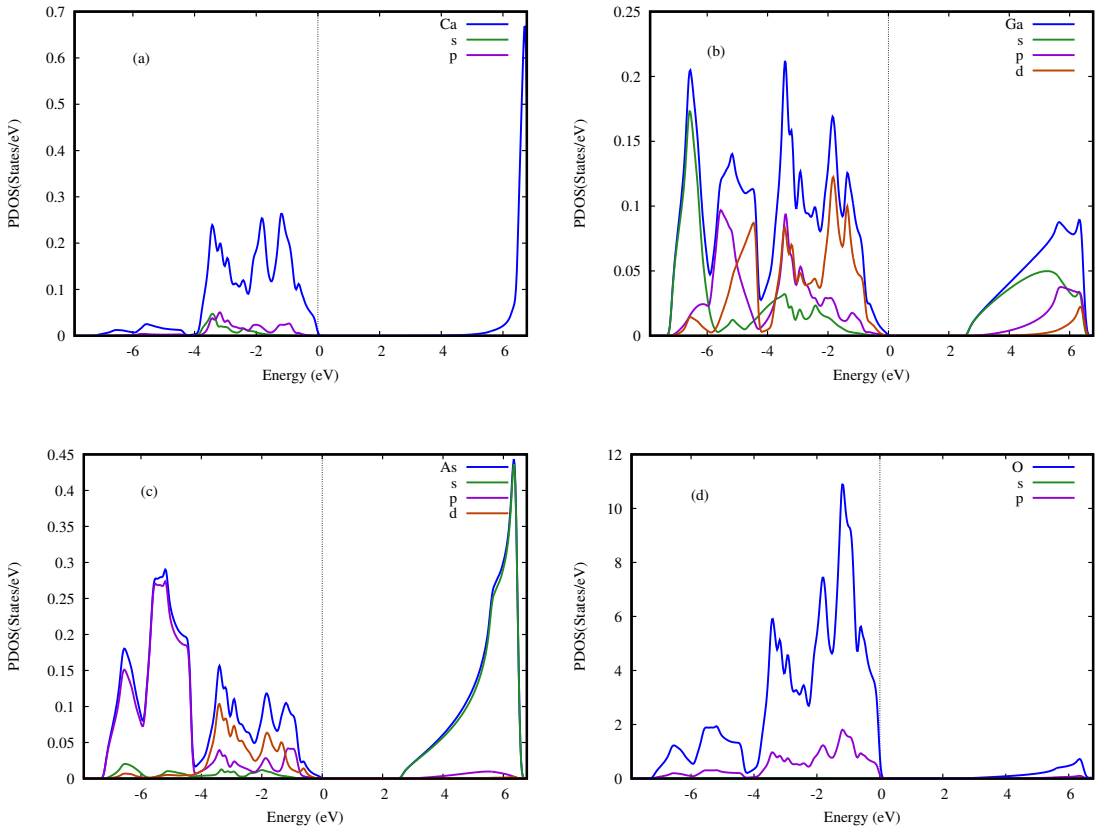

Figure 4.5: The partial density of state (PDOS) projected on the orbits of (a) Ca and (b) Ga atoms of Ca_2GaAsO_6 compound

From Figure 4.5a it can be say that the contribution of the electrons of Ca atoms in the conduction band region is more than the valence band region for both potential,

where the electrons of the s and p orbitals don't contribute significantly. Figure 4.5b shows that most of the electrons of the Ga atom are in the valence band region and the contribution of the electrons of the d orbital is greater than that of the s and p orbitals. We also see that the keen peaks for d and s orbital electrons are near and far from the Fermi energy level, respectively. It is seen that the contribution of s orbital electrons to the conduction band is less than that of the others following the p orbital. From Figure 4.5c, we see that most of the peaks are in the valence band region, but there is also a significant peak in the conduction band region. In the valence band region, p orbital electrons contribute most, followed by d orbital electrons. On the other hand, the contribution of s orbital electrons to the valence band region is way more than the electrons of other orbitals. Now, looking at Figure 4.5d, we can say the electrons of O atoms are mostly occupied in the valence band region rather than the conduction band region, and the electrons of p atoms have a higher concentration than the s ones.

4.4 Optical Properties

The term optical property describes a material's behavior when electromagnetic radiation (light) is incident on the material's surface or, in other words, how a material interacts under an incident electromagnetic radiation. The optical properties of matter are studied in optical physics, a subfield of optics. Different types of material show different optical properties due to differences in physical, chemical, and mechanical characteristics. The knowledge of optical properties is very important in various industrial as well as in scientific applications. In the selection of material for the purpose of contactless temperature measurement devices, heat transfer methods, laser technology, etc., complete knowledge of optical properties of materials is necessary for efficient operation. The optical properties of a material defines how it interacts with light.

4.4.1 Dielectric Function

The correlation between energy band structure and optical transition is expressed by the complex dielectric function of a material. The complex dielectric function of the semiconductor material is

$$\epsilon(\omega) = \epsilon_1(\omega) + i\epsilon_2(\omega) \tag{4.2}$$

The dielectric function can be used to describe how an electromagnetic field affects a material's optical response. The real and imaginary dielectric function for Ca_2GaAsO_6 was obtained from mBJ potential in Figure 4.6 where energy plotted in the X-direction, real and imaginary dielectric function plotted in the Y-direction. This figure represents the curve for real dielectric function. As can be seen in Figure, the curves in these compounds are opposite configurations in the infrared region.

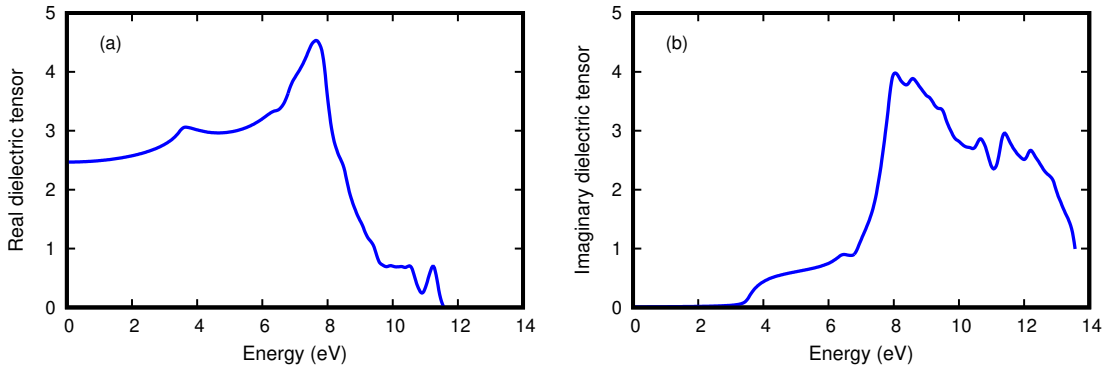

Figure 4.6: (a)Real and (b)imaginary dielectric function of double perovskitess Ca_2GaAsO_6 compound

In Figure 4.6 we can see that the imaginary dielectric tensor is high in the infrared region for Ca_2GaAsO_6 compounds. After the visible region the imaginary dielectric tensor decreasees abruptly. It is introduced as a significant characteristics of a specific crystallographic medium.

4.4.2 Absorption Coefficient

The absorption coefficient is a significant physical property that defines the ability of a material to absorb and reduce the intensity of electromagnetic radiation. Absorption coffiecient helps to measure that a substance can be used for shielding purposes as an anti-reflecting coating. The absorption coffiecient versus energy is illustrated in the following figure by using mBJ potential :

Absorption coffiecient of Ca_2GaAsO_6 compound is in Figure 4.7 :

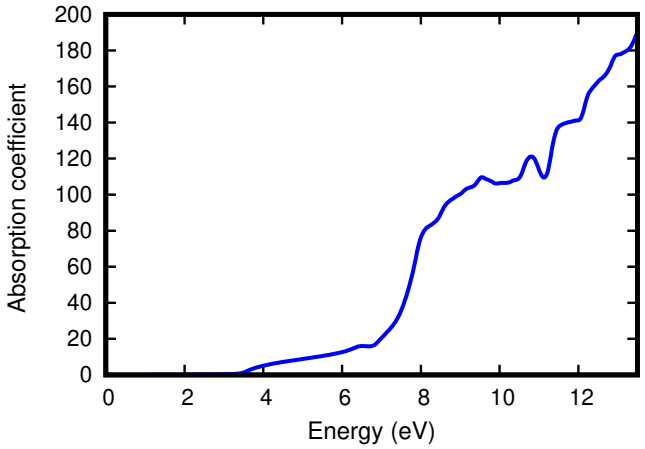

Figure 4.7: Absorption coefficient of double perovskitess Ca_2GaAsO_6 compound

Figure 4.7 shows that although the double perovskites exhibits significant absorption peaks in the ultraviolet region of the electromagnetic spectrum, it also exhibits significant absorption in the visible region of light, making it a good candidate for use in electro-optical applications in the visible region.

4.4.3 Optical Reflectivity and Refractive Index

Material reflectivity is important in determining how much light a material can reflect in relation to the amount of light. The refractive index is known that the refractive indices are inversely related to the bandgap, if the refractive index increases

corresponding band gap decreases. The refractive index can be written as

$$n = \frac{1}{\sqrt{2}}(\sqrt{(Re\epsilon(\omega))^2 + (Im\epsilon(\omega))^2} + (Re\epsilon(\omega))^{\frac{1}{2}} \tag{4.3}$$

Optical reflectivity vs energy curve for double perovskites Ca_2GaAsO_6 is represented in Figure 4.8a for the double perovskitess Ca_2GaAsO_6 :

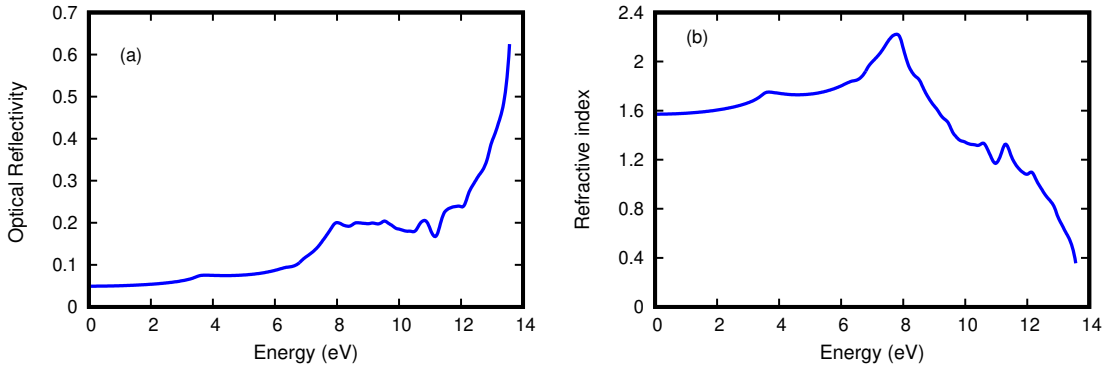

Figure 4.8: (a)Optical reflectivity and (b)refractive Index of double perovskitess Ca_2GaAsO_6

From Figure 4.8a, we can see that the optical reflectivity increase for the increase of energy. In Figure 4.8b, it can be seen that in the lower energy range, there are higher values of refractive index for the compounds. The refractive index increases with the increase in energy and reaches its maximum value of about n = 2.21 at the energy of E = 7.83 eV .

4.4.4 Optical Conductivity

The optical conductivity is one of the crucial metrics used to describe the optical characteristics of solids, and it is primarily employed to identify any potential interband optical transitions that may still be permitted in a given substance. The complex optical conductivity ($\sigma^* = \sigma_1 + i\sigma_2$) is related to the real and imaginary parts (Re$\epsilon(\omega)$, Im$\epsilon(\omega)$) of the complex dielectric function $\epsilon^*(\omega)$ by the following expressions

$$\sigma_1 = \omega\epsilon_2\epsilon_0 \tag{4.4}$$

$$\sigma_1 = \omega\epsilon_2\epsilon_0 \tag{4.5}$$

where ω =$(2\pi\mu)$ is the angular frequency and ($\epsilon_0 = 8.854\times 10^{-12}$ Fm^{-1}) is the free space dielectric constant.

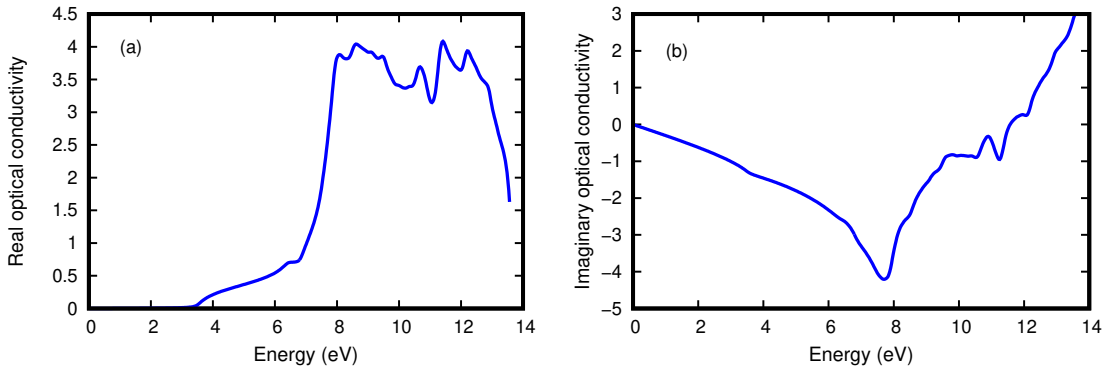

Figure 4.9: (a)Real and (b)imaginary part of optical conductivity for double perovskitess Ca_2GaAsO_6 compound

According to Figure 4.9a, this material exhibits a significant value of σ_1 in the visible area of light, despite the fact that the true component of optical conductivity's most significant peaks emerge in the electro-magnetic field's ultraviolet region. We found that the value of σ_1 is initially zero and remains close to zero in the range from 0.0 eV to 3.34 eV, then increases gradually. Figure 4.9b shows that, at first, the imaginary component of optical conductivity falls with a rise in energy until it reaches a specific point, where it is at its lowest. We found the minimum value to be -4.2 at 7.86 eV. After that minimum value, it increases with increasing energy.

4.4.5 Electron Energy Loss

Energy loss function is the energy lost by a fast-moving electron as it travel through a substance. It's a very significant phase since it offers information about the sample or material's structure.

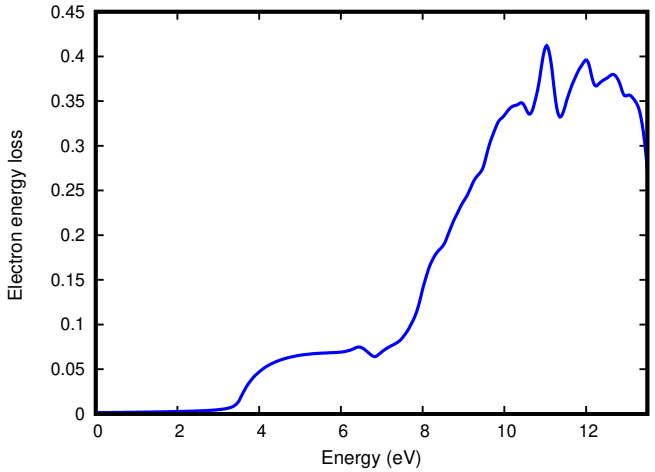

Figure 4.10: Electron energy loss of Ca_2GaAsO_6 compound

The electronic energy loss function of a material can be extended from the dielectric function to further characterize the energy loss when electrons flow through a uniform dielectric. According to the Figure 4.10, as electron energy increases, electron energy loss also increases because of the electrons and atoms in the compound interact. Consequently, the electrons release energy through processes like excitation and ionization. There are numerous picks available in various energies. It is due to the presence of various atoms in our materials.

Chapter 5

Conclusion

The structural, electronic and optical properties of the double perovskites compound Ca_2GaAsO_6 has explored by using first-principles calculations. The electronic band structure of Ca_2GaAsO_6 has examined using density functional theory (DFT) in the context of the modified Becke Johnson (mBJ). Our calculations show that Ca_2GaAsO_6 is a semiconductor with a moderate Γ point direct bandgap of about 2.607 eV, obtained with the modified Becke Johnson (mBJ) potential. It has been determined that the compound exibits direct band-gap characteristics. The density of states has also demonstrated that this compound is a semiconductor. The electrons in Oxygen atoms have been shown to contribute most to the region of the valence band, whereas the electrons in Calcium atoms have been found to contribute most to the region of the conduction band. The optical characteristics display interesting phenomena with good optical absorption in the visible area. By calculating the absorption and emission spectra, we gained insights into the material's ability to absorb and emit light at different energy levels. These optical properties make Ca_2GaAsO_6 a promising candidate for applications in solid-state lighting, photovoltaics, and other optoelectronic devices. Overall, the results presented in this thesis contribute to the comprehensive understanding of Ca_2GaAsO_6 and its potential applications in various technological fields.

However, it is important to note that our study is based on theoretical calculations and assumptions. Future research should focus on computational verification of our findings and the synthesis of Ca_2GaAsO_6 to confirm its predicted properties. Additionally, exploring the influence of doping and alloying on the properties of Ca_2GaAsO_6 could provide further opportunities for tailoring its properties and expanding its range of applications.

In conclusion, this thesis has provided a comprehensive investigation of the structural, electronic and optical properties of Ca_2GaAsO_6 through a first-principles study. The results presented here not only deepen our understanding of this double perovskites compound but also contribute to the broader field of materials science. The findings pave the way for future research and development in the design of novel materials for advanced electronic and optoelectronic applications.

Chapter 6

List of Abbreviations

BZ	:	Brillouin Zone
DFT	:	Density Functional Theory
DOS	:	Density of States
GGA	:	Generalized Gradient Approximation
HK	:	Hohenberg-Kohn
KS	:	Kohn-Sham
LSDA	:	Local Spin Density Approximation
SOC	:	Spin Orbit Coupling
XC	:	Exchange correlation
GMR	:	Giant Magnetoresistance
EM	:	Electro Magnetic
NM	:	Non Magnetic
DOS	:	Density of States
PDOS	:	Partial Density of States
AF	:	Antiferromagnetic
NMR	:	Nuclear Magnetic Resonance

Bibliography

[1] Wan-Jian Yin, Baicheng Weng, Jie Ge, Qingde Sun, Zhenzhu Li, and Yanfa Yan. Oxide perovskites, double perovskites and derivatives for electrocatalysis, photocatalysis, and photovoltaics. *Energy Environ. Sci.*, 12(2):442–462, 2019.

[2] Xiaoyun Chen, Jun Xu, Yueshan Xu, Feng Luo, and Yaping Du. Rare earth double perovskites: a fertile soil in the field of perovskite oxides. *Inorg. Chem. Front.*, 6(9):2226–2238, 2019.

[3] Sajad Ahmad Dar, Malak Azmat Ali, and Vipul Srivastava. Investigation on bismuth-based oxide perovskites mbio 3 (m= rb, cs, tl) for structural, electronic, mechanical and thermal properties. *The European Physical Journal B*, 93:1–11, 2020.

[4] Xin-Gang Zhao, Dongwen Yang, Ji-Chang Ren, Yuanhui Sun, Zewen Xiao, and Lijun Zhang. Rational design of halide double perovskites for optoelectronic applications. *Joule*, 2(9):1662–1673, 2018.

[5] Malak Azmat Ali, Thamraa Alshahrani, and G Murtaza. Defective perovskites cs2secl6 and cs2tecl6 as novel high temperature potential thermoelectric materials. *Mater. Sci. Semicond.*, 127:105728, 2021.

[6] H Benmhidi, H Rached, D Rached, and M Benkabou. Ab initio study of electronic structure, elastic and transport properties of fluoroperovskite libef. *Journal of Electronic Materials*, 46(4), 2017.

[7] Pierre Hohenberg and Walter Kohn. Inhomogeneous electron gas. *Phys. Rev. E .*, 136(3B):B864, 1964.

[8] AV Kosobutsky and Yu M Basalaev. First principles study of electronic structure and optical properties of limte2 (m= al, ga, in) crystals. *J. Phys. Chem.*, 71(5):854–861, 2010.

[9] Herbert Needleman. Lead poisoning. *Annu. Rev. Med.*, 55:209–222, 2004.

[10] Sami Vasala and Maarit Karppinen. A2b b o6 perovskites: a review. *Prog. Solid. State Ch.*, 43(1-2):1–36, 2015.

[11] K-I Kobayashi, T Kimura, H Sawada, K Terakura, and Y Tokura. Room-temperature magnetoresistance in an oxide material with an ordered double-perovskite structure. *Nature*, 395(6703):677–680, 1998.

[12] DD Sarma. A new class of magnetic materials: Sr2femoo6 and related compounds. *Solid State Commun*, 5(4):261–268, 2001.

[13] B Garcıa-Landa, C Ritter, MR Ibarra, J Blasco, PA Algarabel, R Mahendiran, and J Garcıa. Magnetic and magnetotransport properties of the ordered perovskite sr2femoo6. *Solid State Commun*, 110(8):435–438, 1999.

[14] DD Sarma, EV Sampathkumaran, Sugata Ray, R Nagarajan, Subham Majumdar, Ashwani Kumar, G Nalini, and TN Guru Row. Magnetoresistance in ordered and disordered double perovskite oxide, sr2femoo6. *Solid State Commun*, 114(9):465–468, 2000.

[15] Zhiming Wang, Ye Tian, and Yongdan Li. Direct ch4 fuel cell using sr2femoo6 as an anode material. *J. Power Sources*, 196(15):6104–6109, 2011.

[16] Shun Li, Bandar AlOtaibi, Wei Huang, Zetian Mi, Nick Serpone, Riad Nechache, and Federico Rosei. Epitaxial bi2fecro6 multiferroic thin film as a new visible light absorbing photocathode material. *Small*, 11(32):4018–4026, 2015.

[17] Riad Nechache, Cristian Victor Cojocaru, Catalin Harnagea, Christian Nauenheim, Mischa Nicklaus, Andreas Ruediger, Federico Rosei, and Alain Pignolet. Epitaxial patterning of bi2fecro6 double perovskite nanostructures: multiferroic at room temperature. *Adv Mater*, 23(15):1724–1729, 2011.

[18] Shun Li, Bandar AlOtaibi, Wei Huang, Zetian Mi, Nick Serpone, Riad Nechache, and Federico Rosei. Epitaxial bi2fecro6 multiferroic thin film as

a new visible light absorbing photocathode material. *Small*, 11(32):4018–4026, 2015.

[19] Riad Nechache, Cristian Victor Cojocaru, Catalin Harnagea, Christian Nauenheim, Mischa Nicklaus, Andreas Ruediger, Federico Rosei, and Alain Pignolet. Epitaxial patterning of bi2fecro6 double perovskite nanostructures: multiferroic at room temperature. *Adv. Mater. Technol.*, 23(15):1724–1729, 2011.

[20] Nyrissa S Rogado, Jun Li, Arthur W Sleight, and Mas A Subramanian. Magnetocapacitance and magnetoresistance near room temperature in a ferromagnetic semiconductor: La2nimno6. *Adv. Mater. Technol.*, 17(18):2225–2227, 2005.

[21] CL Bull, D Gleeson, and KS Knight. Determination of b-site ordering and structural transformations in the mixed transition metal perovskites la2comno6 and la2nimno6. *J. Phys. Condens.*, 15(29):4927, 2003.

[22] YQ Lin, XM Chen, and XQ Liu. Relaxor-like dielectric behavior in la2nimno6 double perovskite ceramics. *Solid State Commun*, 149(19-20):784–787, 2009.

[23] J Alvarado-Flores and L Ávalos-Rodríguez. Materiales para ánodos, cátodos y electrolitos utilizados en celdas de combustible de óxido sólido (sofc). *Supl. Rev. Mex. Fis*, 59(1):66–87, 2013.

[24] K Kuepper, I Balasz, H Hesse, A Winiarski, KC Prince, M Matteucci, D Wett, R Szargan, E Burzo, and M Neumann. Electronic and magnetic properties of highly ordered sr2femoo6. *Phys. Status Solidi*, 201(15):3252–3256, 2004.

[25] K-W Lee and WE Pickett. Sr2vo3feas: a nanolayered bimetallic iron pnictide superconductor. *EPL*, 89(5):57008, 2010.

[26] Jong Mok Ok, S-H Baek, C Hoch, RK Kremer, SY Park, Sungdae Ji, B Büchner, J-H Park, SI Hyun, JH Shim, et al. Frustration-driven c 4 symmetric order in a naturally-heterostructured superconductor sr2vo3feas. *Nat. Commun.*, 8(1):2167, 2017.

[27] KD Nelson, ZQ Mao, Y Maeno, and Ying Liu. Odd-parity superconductivity in sr2ruo4. *Science*, 306(5699):1151–1154, 2004.

[28] Ying Liu and Zhi-Qiang Mao. Unconventional superconductivity in sr2ruo4. *Physica C Supercond*, 514:339–353, 2015.

[29] G Ml Luke, Y Fudamoto, KM Kojima, MI Larkin, J Merrin, B Nachumi, YJ Uemura, Y Maeno, ZQ Mao, Y Mori, et al. Time-reversal symmetry-breaking superconductivity in sr2ruo4. *Nature*, 394(6693):558–561, 1998.

[30] D.J. Griffiths. *Introduction to Quantum Mechanics*. Cambridge University Press, 2017.

[31] Hermann Weyl. Quantenmechanik und gruppentheorie. *Z Med Phys*, 46(1-2):1–46, 1927.

[32] David J Griffiths and Darrell F Schroeter. *Introduction to quantum mechanics*. Cambridge J. Reg. Econ., 2018.

[33] Wolfram Koch and Max C Holthausen. *A chemist's guide to density functional theory*. John Wiley & Sons, 2015.

[34] Arthur Jabs. Connecting spin and statistics in quantum mechanics. *Found Phys*, 40:776–792, 2010.

[35] Wolfgang Pauli. Über den zusammenhang des abschlusses der elektronengruppen im atom mit der komplexstruktur der spektren. *Einführ. Orig*, 229:765–783, 1925.

[36] Klaus Capelle. A bird's-eye view of density-functional theory. *Braz. J. Phys.*, 36:1318–1343, 2006.

[37] Ville J Härkönen, Robert van Leeuwen, and Eberhard KU Gross. Many-body green's function theory of electrons and nuclei beyond the born-oppenheimer approximation. *Phys. Rev. B*, 101(23):235153, 2020.

[38] Jean-Michel Combes, Pierre Duclos, and Ruedi Seiler. The born-oppenheimer approximation. *Rigorous atomic and molecular physics*, pages 185–213, 1981.

[39] Hanno Essén. The physics of the born–oppenheimer approximation. *Int J Quantum Chem*, 12(4):721–735, 1977.

[40] Paul Adrien Maurice Dirac. A new notation for quantum mechanics. In *Mathematical Proceedings of the Cambridge Philosophical Society*, volume 35, pages 416–418. Cambridge University Press, 1939.

[41] Wolfram Koch and Max C Holthausen. *A chemist's guide to density functional theory*. John Wiley & Sons, 2015.

[42] John D Goddard, Nicholas C Handy, and Henry F Schaefer III. Gradient techniques for open-shell restricted hartree–fock and multiconfiguration self-consistent-field methods. *J. Chem. Phys.*, 71(4):1525–1530, 1979.

[43] Asger Halkier, Trygve Helgaker, Poul Jørgensen, Wim Klopper, and Jeppe Olsen. Basis-set convergence of the energy in molecular hartree–fock calculations. *Chem. Phys. Lett.*, 302(5-6):437–446, 1999.

[44] Philippe C Hiberty, Stephane Humbel, David Danovich, and Sason Shaik. What is physically wrong with the description of odd-electron bonding by hartree-fock theory? a simple nonempirical remedy. *J. Am. Chem. Soc.*, 117(35):9003–9011, 1995.

[45] Ida Josefsson, Kristjan Kunnus, Simon Schreck, Alexander Fohlisch, Frank de Groot, Philippe Wernet, and Michael Odelius. Ab initio calculations of x-ray spectra: Atomic multiplet and molecular orbital effects in a multiconfigurational scf approach to the l-edge spectra of transition metal complexes. *J. Phys. Chem.*, 3(23):3565–3570, 2012.

[46] John C Slater. A simplification of the hartree-fock method. *Phys. Rev. E.*, 81(3):385, 1951.

[47] Wolfgang Pauli. The connection between spin and statistics. *Phys. Rev. E .*, 58(8):716, 1940.

[48] A Szabo and NS Ostlund. Modern quantum chemistry, revised 1st edition. 1989.

[49] F Schwabl. Quantum mechanics (qm i). ; quantenmechanik (qm i). eine einfuehrung. 2007.

[50] Pierre Hohenberg and Walter Kohn. Inhomogeneous electron gas. *Phys. Rev. E.*, 136(3B):B864, 1964.

[51] DWJ Cruickshank. The accuracy of electron-density maps in x-ray analysis with special reference to dibenzyl. *Acta Crystallogr.*, 2(2):65–82, 1949.

[52] WD Myers and WJ Swiatecki. Nuclear properties according to the thomas-fermi model. *Nucl. Phys.*, 601(2):141–167, 1996.

[53] WD Myers and WJ Swiatecki. A thomas-fermi model of nuclei. part i. formulation and first results. *Ann Phys (N Y)*, 204(2):401–431, 1990.

[54] John Ferreirinho, Remo Ruffini, and Luigi Stella. On the relativistic thomas-fermi model. *Mod Phys Lett B*, 91(2):314–316, 1980.

[55] Erwin Schrödinger. An undulatory theory of the mechanics of atoms and molecules. *Phys. Rev. E .*, 28(6):1049, 1926.

[56] Somayeh F Rastegar, Nasser L Hadipour, and Hamed Soleymanabadi. Theoretical investigation on the selective detection of so 2 molecule by aln nanosheets. *J. Mol. Model.*, 20:1–6, 2014.

[57] Somayeh F Rastegar, Nasser L Hadipour, Mohammad Bigdeli Tabar, and Hamed Soleymanabadi. Dft studies of acrolein molecule adsorption on pristine and al-doped graphenes. *J. Mol. Model.*, 19:3733–3740, 2013.

[58] JA Camargo-Martínez and R Baquero. Performance of the modified becke-johnson potential for semiconductors. *Phys. Rev. B*, 86(19):195106, 2012.

[59] JA Camargo-Martínez and R Baquero. The modified becke-johnson potential analyzed. *Superf. y Vacio*, 26(2):54–57, 2013.

[60] Gang Bao, Guanghui Hu, and Di Liu. Numerical solution of the kohn-sham equation by finite element methods with an adaptive mesh redistribution technique. *J. Sci. Comput.*, 55:372–391, 2013.

[61] Huajie Chen, Xingao Gong, Lianhua He, Zhang Yang, and Aihui Zhou. Numerical analysis of finite dimensional approximations of kohn–sham models. *Adv Comput Math*, 38(2):225–256, 2013.

[62] Klaus Capelle. A bird's-eye view of density-functional theory. *Braz. J. Phys.*, 36:1318–1343, 2006.

[63] Om P Agrawal. Formulation of euler–lagrange equations for fractional variational problems. *J. Math. Anal. Appl.*, 272(1):368–379, 2002.

[64] John P Perdew, Huy Q Tran, and Elizabeth D Smith. Stabilized jellium: Structureless pseudopotential model for the cohesive and surface properties of metals. *Physical Review B*, 42(18):11627, 1990.

[65] Zenebe Assefa Tsegaye. Density functional theory studies of electronic and optical properties of zns alloyed with mn and cr. Master's thesis, Institutt for fysikk, 2012.

[66] Matthias Ernzerhof and Gustavo E Scuseria. Assessment of the perdew–burke–ernzerhof exchange-correlation functional. *J. Chem. Phys.*, 110(11):5029–5036, 1999.

[67] Philipp Haas, Fabien Tran, Peter Blaha, and Karlheinz Schwarz. Construction of an optimal gga functional for molecules and solids. *Phys. Rev. B*, 83(20):205117, 2011.

[68] MD Segall, Philip JD Lindan, MJ al Probert, Christopher James Pickard, Philip James Hasnip, SJ Clark, and MC Payne. First-principles simulation: ideas, illustrations and the castep code. *J. Phys. Condens*, 14(11):2717, 2002.

[69] Somayeh F Rastegar, Nasser L Hadipour, and Hamed Soleymanabadi. Theoretical investigation on the selective detection of so 2 molecule by aln nanosheets. *J. Mol. Model.*, 20:1–6, 2014.

[70] Denis Music, Richard W Geyer, and Jochen M Schneider. Recent progress and new directions in density functional theory based design of hard coatings. *Surf. Coat. Technol.*, 286:178–190, 2016.

[71] M Hussein Assadi, Dorian AH Hanaor, et al. Theoretical study on copper's energetics and magnetism in tio2 polymorphs. *J. Appl. Phys.*, 113(23), 2013.

[72] Somayeh F Rastegar, Nasser L Hadipour, Mohammad Bigdeli Tabar, and Hamed Soleymanabadi. Dft studies of acrolein molecule adsorption on pristine and al-doped graphenes. *J. Mol. Model.*, 19:3733–3740, 2013.

[73] Pierre Hohenberg and Walter Kohn. Inhomogeneous electron gas. *Phys. Rev. Lett.*, 136(3B):B864, 1964.

[74] John P Perdew, Kieron Burke, and Matthias Ernzerhof. Generalized gradient approximation made simple. *Phys. Rev. E*, 77(18):3865, 1996.

[75] AV Kosobutsky and Yu M Basalaev. First principles study of electronic structure and optical properties of limte2 (m= al, ga, in) crystals. *J. Phys. Chem.*, 71(5):854–861, 2010.

[76] Walter Heitler and Fritz London. Wechselwirkung neutraler atome und homöopolare bindung nach der quantenmechanik. *Z Med Phys*, 44(6-7):455–472, 1927.

[77] Richard M Martin. *Electronic structure: basic theory and practical methods*. Cambridge university press, 2020.

[78] Lianshan Lin. Materials databases infrastructure constructed by first principles calculations: A review. *Mater. Perform. Charact.*, 4(1), 2015.

[79] Anubhav Jain, Shyue Ping Ong, Geoffroy Hautier, Wei Chen, William Davidson Richards, Stephen Dacek, Shreyas Cholia, Dan Gunter, David Skinner, Gerbrand Ceder, et al. Commentary: The materials project: A materials genome approach to accelerating materials innovation. *APL Mater*, 1(1):011002, 2013.